Determination of the strong coupling constant $\alpha_S(m_Z)$ from measurements of inclusive $W^{\pm}$ and Z boson production cross sections in proton-proton collisions at $\sqrt{s} = 7$ and 8 TeV

CMS Collaboration ; Canelli, M Florencia ; Kilminster, Benjamin ; Caminada, Lea ; Botta, Cristina ; Aarrestad, Thea K ; Brzhechko, Danyyl ; De Cosa, Annapaoloa ; Del Burgo, Riccardo ; Donato, Silvio ; Heikkilä, Jaana K ; Leontsinis, Stefanos ; Mikuni, Vinicius Massami ; Missiroli, Marino ; Neutelings, Izaak ; Rauco, Giorgia ; Robmann, Peter ; Schweiger, Korbinian ; Takahashi, Yuta ; Wertz, Sebastien ; Zucchetta, Alberto ; et al

DOI: https://doi.org/10.1007/JHEP06(2020)018

Published for SISSA by Springer

Received: *December 9, 2019*
Accepted: *April 29, 2020*
Published: *June 1, 2020*

Determination of the strong coupling constant $\alpha_S(m_Z)$ from measurements of inclusive $W^{\pm}$ and Z boson production cross sections in proton-proton collisions at $\sqrt{s} = 7$ and 8 TeV

The CMS collaboration

E-mail: cms-publication-committee-chair@cern.ch

Abstract: Twelve measurements of inclusive cross sections of $W^{\pm}$ and Z boson production, performed in proton-proton collisions at centre-of-mass energies of 7 and 8 TeV, are compared with perturbative quantum chromodynamics calculations at next-to-next-to-leading order (NNLO) accuracy obtained with the CT14, HERAPDF2.0, MMHT14, and NNPDF3.0 parton distribution functions (PDFs). Data and theory agree well for all PDF sets, taking into account the experimental and theoretical uncertainties. A novel procedure is employed to extract the strong coupling constant at the Z pole mass from a detailed comparison of all the experimental fiducial cross sections to the corresponding NNLO theoretical predictions, yielding $\alpha_S(m_Z) = 0.1163^{+0.0024}_{-0.0031}$ (CT14), $0.1072^{+0.0043}_{-0.0040}$ (HERAPDF2.0), 0.1186 ± 0.0025 (MMHT14), and 0.1147 ± 0.0023 (NNPDF3.0). Using the results obtained with the CT14 and MMHT14 PDFs, which yield the most robust and stable $\alpha_S(m_Z)$ extractions, a value $\alpha_S(m_Z) = 0.1175^{+0.0025}_{-0.0028}$ is determined.

Keywords: Hadron-Hadron scattering (experiments), Particle and resonance production

ArXiv ePrint: 1912.04387

https://doi.org/10.1007/JHEP06(2020)018

JHEP06(2020)018

Contents

JHEP06(2020)018

1 Introduction

In the chiral limit of zero quark masses, the α_S coupling is the only free parameter of quantum chromodynamics (QCD), the theory of the strong interaction between quarks and gluons. Because of its logarithmic decrease with energy (asymptotic freedom), α_S is commonly given at a reference scale, often taken at the Z pole mass. Its current value, $\alpha_S(m_Z) = 0.1181 \pm 0.0011$, is known with a $\pm 0.9\%$ uncertainty, making it the least precisely known of all interaction couplings in nature [1]. The precision of the strong coupling value plays an important role in all theoretical calculations of perturbative QCD (pQCD) processes involving partons, and currently leads to 3–7% uncertainties in key Higgs boson processes, such as the cross sections for gluon-gluon fusion ($gg \to H$) and associated production with a top quark pair ($t\bar{t}H$), as well as the $H \to b\bar{b}, c\bar{c}, gg$ partial decay widths [2]. As one of the fundamental parameters of the standard model (SM), the uncertainties of the QCD coupling value also dominate the propagated parametric uncertainties in the theoretical calculations of the top quark mass [3], as well as of electroweak (EW) precision observables [4]. Last but not least, α_S also impacts physics approaching the Planck scale,

Measurement	Fiducial cross section
pp at $\sqrt{s} = 7$ TeV [13]	
W^+_e, $p^e_T > 25$ GeV, $\lvert\eta^e\rvert < 2.5$	3404 ± 12 (stat) ± 67 (syst) ± 136 (lumi) pb $= 3404 \pm 152$ pb
W^-_e, $p^e_T > 25$ GeV, $\lvert\eta^e\rvert < 2.5$	2284 ± 10 (stat) ± 43 (syst) ± 91 (lumi) pb $= 2284 \pm 101$ pb
Z_e, $p^e_T > 25$ GeV, $\lvert\eta^e\rvert < 2.5$, $60 < m_Z < 120$ GeV	452 ± 5 (stat) ± 10 (syst) ± 18 (lumi) pb $= 452 \pm 21$ pb
W^+_μ, $p^\mu_T > 25$ GeV, $\lvert\eta^\mu\rvert < 2.1$	2815 ± 9 (stat) ± 42 (syst) ± 113 (lumi) pb $= 2815 \pm 121$ pb
W^-_μ, $p^\mu_T > 25$ GeV, $\lvert\eta^\mu\rvert < 2.1$	1921 ± 8 (stat) ± 27 (syst) ± 77 (lumi) pb $= 1921 \pm 82$ pb
Z_μ, $p^\mu_T > 20$ GeV, $\lvert\eta^\mu\rvert < 2.1$, $60 < m_Z < 120$ GeV	396 ± 3 (stat) ± 7 (syst) ± 16 (lumi) pb $= 396 \pm 18$ pb
pp at $\sqrt{s} = 8$ TeV [14]	
W^+_e, $p^e_T > 25$ GeV, $\lvert\eta^e\rvert < 1.44$, $1.57 < \lvert\eta^e\rvert < 2.5$	3540 ± 20 (stat) ± 110 (syst) ± 90 (lumi) pb $= 3540 \pm 140$ pb
W^-_e, $p^e_T > 25$ GeV, $\lvert\eta^e\rvert < 1.44$, $1.57 < \lvert\eta^e\rvert < 2.5$	2390 ± 10 (stat) ± 60 (syst) ± 60 (lumi) pb $= 2390 \pm 90$ pb
Z_e, $p^e_T > 25$ GeV, $\lvert\eta^e\rvert < 1.44$, $1.57 < \lvert\eta^e\rvert < 2.5$, $60 < m_Z < 120$ GeV	450 ± 10 (stat) ± 10 (syst) ± 10 (lumi) pb $= 450 \pm 20$ pb
W^+_μ, $p^\mu_T > 25$ GeV, $\lvert\eta^\mu\rvert < 2.1$	3100 ± 10 (stat) ± 40 (syst) ± 80 (lumi) pb $= 3100 \pm 90$ pb
W^-_μ, $p^\mu_T > 25$ GeV, $\lvert\eta^\mu\rvert < 2.1$	2240 ± 10 (stat) ± 20 (syst) ± 60 (lumi) pb $= 2240 \pm 60$ pb
Z_μ, $p^\mu_T > 25$ GeV, $\lvert\eta^\mu\rvert < 2.1$, $60 < m_Z < 120$ GeV	400 ± 10 (stat) ± 10 (syst) ± 10 (lumi) pb $= 400 \pm 20$ pb

Table 1. Summary of the twelve $W^\pm$ and Z boson production cross sections, along with their individual (and total, added in quadrature) uncertainties, measured with the indicated fiducial selection criteria on the transverse momentum (p^ℓ_T) and pseudorapidity (η^ℓ), in the electron ($W^\pm{}_e$, Z_e) and muon ($W^\pm{}_\mu$, Z_μ) final states, in pp collisions at $\sqrt{s} = 7$ and 8 TeV [13, 14].

either through the EW vacuum stability [5], or in searches of new coloured sectors that may modify its running towards the grand unification scale [6, 7].

The current $\alpha_S(m_Z)$ world-average value is derived from a combination of six subclasses of (mostly) independent observables measured at various energy scales, which are compared with pQCD calculations at next-to-next-to-leading order (NNLO), or beyond, accuracy [1]. The only hadron collider observable so far that provides a constraint on α_S at this level of theoretical accuracy is the total $t\bar{t}$ cross section [8–10]. One of the paths towards improvement of our knowledge of the QCD coupling is the inclusion into the world average of new independent observables sensitive to α_S that are experimentally and theoretically known with high precision [11, 12]. Charged- and neutral-current Drell-Yan processes in their leptonic decay modes, $pp \to W^\pm \to \ell^\pm \nu_\ell$ and $pp \to Z \to \ell^+\ell^-$ with $\ell^\pm = e^\pm, \mu^\pm$, are the most accurately known processes currently accessible in proton-proton (pp) collisions at the CERN LHC. Experimentally, the uncertainties in the inclusive $V = W^\pm, Z$ production cross sections measured by the CMS experiment are between 3 and 5%; these are dominated by the integrated luminosity uncertainty, whereas the statistical uncertainties are at the subpercent level (table 1) [13, 14]. On the theoretical side, the corresponding cross sections are known at NNLO pQCD accuracy [15], with about 1–4% parton distribution function (PDF), and 0.3–1.3% scale uncertainties [16]. Electroweak corrections, which lead to a few percent reduction of the pure-pQCD $W^\pm$ and Z boson production cross sections, are known at next-to-leading order (NLO) accuracy [17].

Theoretical calculations [18] indicate that about one fourth of the total V production cross sections at LHC energies come from partonic processes beyond the Born level, and thereby depend on the QCD coupling value. By calculating the V production cross sections at NNLO for varying $\alpha_S(m_Z)$ values, and by comparing the theoretical predictions to experimental data, one can therefore derive a value of the strong coupling constant at the Z pole, independent of other current extractions [19]. By combining such a result with those derived from other methods, the overall uncertainty in the $\alpha_S(m_Z)$ world average

JHEP06(2020)018

can eventually be reduced. The use of inclusive $W^{\pm}$, Z boson cross sections to extract the QCD coupling is presented here for the first time. This method is similar to the one used to extract α_S from the inclusive $t\bar{t}$ cross sections at hadron colliders [8–10], except that the underlying physical process is quite different. Whereas $\sigma(t\bar{t})$ depends on α_S already at leading order (LO), albeit with ≈5% theoretical and experimental uncertainties, $\sigma(V)$ is more precisely known experimentally and theoretically, although at the Born level its underlying partonic processes are purely EW with a dependence on α_S that comes only through higher-order pQCD corrections (at LO, the $\sigma(V)$ cross sections also depend on α_S via the PDFs).

The paper is organised as follows. The experimental setup used in the twelve CMS original measurements is summarised in section 2. In section 3, the theoretical tools used to perform the calculations are outlined. In section 4, the experimental and theoretical cross sections with associated uncertainties, are compared. In section 5, the method to extract $\alpha_S(m_Z)$ from the data-to-theory comparison for each measurement is described, as well as the approach to combine all $\alpha_S(m_Z)$ estimates into a single value per PDF set that properly takes into account the experimental and theoretical uncertainties and their correlations. The final $\alpha_S(m_Z)$ values derived are presented and discussed in section 6. The work is summarised in section 7.

2 The CMS detector

The results presented here are based on a phenomenological study of $W^{\pm}$ and Z boson fiducial cross sections measured by the CMS experiment in pp collisions at centre-of-mass (c.m.) energies of $\sqrt{s} = 7$ and 8 TeV with integrated luminosities of 38.0 and 18.2 pb^{-1}, respectively [13, 14]. The experimental and theoretical EW boson production cross sections quoted in the whole paper are to be understood as multiplied by their associated leptonic branching fractions, but for simplicity are referred to as "cross sections" hereafter. The final states of interest are those with decay charged leptons (electrons or muons) passing the acceptance criteria listed in table 1.

The central feature of the CMS apparatus is a superconducting solenoid, of 6 m internal diameter, providing a magnetic field of 3.8 T. Within the field volume are a silicon pixel and strip tracker, a crystal electromagnetic calorimeter (ECAL), and a brass and scintillator hadron calorimeter. Electrons with $p_T > 25$ GeV are identified as clusters of energy deposits in the ECAL matched to tracks measured with the silicon tracker. The ECAL fiducial region is defined by $|\eta| < 1.44$ (barrel) or $1.57 < |\eta| < 2.5$ (endcap), where η is the pseudorapidity of the energy cluster. Muons are measured in gas-ionisation detectors embedded in the steel flux-return yoke of the magnet. Muons with $p_T > 20$ or 25 GeV and $|\eta| < 2.1$ are selected in the analyses. Details of the CMS detector and its performance can be found elsewhere [20].

3 Theoretical calculations

According to the pQCD factorisation theorem [21], the cross section for the production of a heavy elementary particle in pp collisions can be calculated through the convolution of

JHEP06(2020)018

matrix elements for the relevant parton-parton subprocesses, computed at a given order in the α_S expansion evaluated at a renormalisation scale μ_R, and a universal nonperturbative part describing the parton density at the factorisation energy scale μ_F and parton fractional momentum x_i in the proton. The production cross section of an EW boson can be written

$$\sigma(\mathrm{pp} \to \mathrm{V{+}X}) = \iint \mathrm{d}x_1 \mathrm{d}x_2 \, f_1(x_1, \mu_F) f_2(x_2, \mu_F) \, \left[\hat{\sigma}_{\mathrm{LO}} + \hat{\sigma}_{\mathrm{NLO}}(\alpha_S(\mu_R)) + \hat{\sigma}_{\mathrm{NNLO}}(\alpha_S(\mu_R)) + \cdots\right],$$

where the functions f_i represent the PDFs of each proton, determined from experimental data, and the expression in brackets is the perturbative expansion of the underlying partonic cross sections $\hat{\sigma}$. At hadron colliders, the LO production of $\mathrm{W}^{\pm}$ and Z bosons involves the annihilation of a quark-antiquark pair of the same ($\mathrm{q\overline{q}} \to \mathrm{Z} + \mathrm{X}$) or different ($\mathrm{q\overline{q}}' \to \mathrm{W} + \mathrm{X}$) flavour. At NLO, the Born terms are supplemented with initial-state real gluon emission, virtual gluon exchange, and contributions from gluon-quark and gluon-antiquark scattering processes. At NNLO, additional gluon radiation and virtual exchanges further contribute to the total cross section [15, 18]. Although at LO the partonic cross sections are independent of α_S, the vertices of the higher-order terms introduce a dependence on α_S that enables the determination of the QCD coupling by comparing high-precision theoretical calculations to the experimental data. The size of such higher-order corrections [19], encoded in the so-called K-factor, amounts to $K = \sigma_{\mathrm{NNLO}}/\sigma_{\mathrm{LO}} \approx 1.25$–$1.37$ as derived with MCFM v.8.0 [16] for the $\mathrm{W}^{\pm}$ and Z cross sections measured at 7 and 8 TeV in the CMS fiducial acceptance, and indicates that EW boson production is indeed sensitive to $\alpha_S(m_Z)$ at NNLO accuracy.

In this work, the NNLO cross sections are computed with the MCFM code interfaced with LHAPDF v.6.1.6 [22] to access four different PDFs: CT14 [23], HERAPDF2.0 [24], MMHT14 [25], and NNPDF3.0 [26]. All these PDFs use as the default central set the one with the QCD coupling constant fixed to $\alpha_S(m_Z) = 0.118$ in their global fits of the data, but also provide a variety of alternative sets with their corresponding central values derived for different fixed values of $\alpha_S(m_Z)$. We note, however, that when the QCD coupling constant is left free in their NNLO PDF fits, the following values are preferred by the different PDF sets: $\alpha_S(m_Z) = 0.115$ (CT14) [23], 0.108 (HERAPDF2.0) [24], and 0.1172 (MMHT2014) [25]. The HERAPDF2.0 set is obtained from fits to HERA deep inelastic scattering (DIS) data only. The CT14, MMHT14, and NNPDF3.0 global fits have been obtained including DIS, fixed target, and LHC measurements. These latter PDF sets incorporate one or two $\mathrm{W}^{\pm}$ or Z differential CMS distributions at 7 TeV [13] in their global fits, but did not use any of the twelve *absolute* inclusive EW boson cross sections listed in table 1, and therefore the corresponding values of α_S extracted here are truly independent of the data contributing to the extraction of PDF sets themselves. The so-called G_μ electroweak scheme, where the input parameters are m_W, m_Z, and G_F, is used in all the predictions. The leptonic W and Z branching fractions are obtained in MCFM from the theoretical leptonic width (computed at LO in electroweak accuracy) normalized to the total W and Z widths experimentally measured [1]. All numerical results have been obtained using the latest SM parameters for particle masses, widths, and couplings [1]. For simplicity, the default value of the charm quark mass in MCFM and NNPDF3.0, $m_c = 1.275$ GeV,

JHEP06(2020)018

is used for all the calculations — rather than the preferred values of the other PDF sets: $m_c = 1.3\,\text{GeV}$ (CT14), 1.43 GeV (HERAPDF2.0), 1.4 GeV (MMHT14) — because the computed cross sections vary only by a few per mille, within the MCFM numerical uncertainty.

The default renormalisation and factorisation scales are set to the corresponding EW boson mass for each process, $\mu = \mu_F = \mu_R = m_W, m_Z$. For all PDF sets, we computed the NNLO cross sections at various $\alpha_S(m_Z)$ values over the range [0.115–0.121]. For NNPDF3.0, the available values are $\alpha_S(m_Z) = 0.115$, 0.117, 0.118, 0.119, and 0.121; and for the other PDF sets they are $\alpha_S(m_Z) = 0.115$, 0.116, 0.117, 0.118, 0.119, 0.120, and 0.121. Technically, the central sets selected via LHAPDF for this study are: CT14nnlo_as_0*iii* (for *iii* = 115–121), HERAPDF20_NNLO_ALPHAS_*iii* (for *iii* = 115–121), MMHT2014nnlo_asmzlargerange (with $\alpha_S(m_Z) = 0.115, \ldots, 0.121$ grids), and NNPDF30_nnlo_as_0*iii* (with *iii* = 115–121). For the PDF uncertainties, only NNPDF3.0 provides independent replicas for each $\alpha_S(m_Z)$ set, which we use in our calculations and uncertainties propagation, whereas the rest of PDFs use the same eigenvalues corresponding to the set determined with $\alpha_S(m_Z) = 0.118$. Calculations are carried out implementing the fiducial selection criteria for the final-state charged leptons corresponding to each of the six different measurements (W_e^+, W_e^-, Z_e, W_μ^+, W_μ^-, Z_μ) at $\sqrt{s} = 7$ and 8 TeV listed in table 1, thereby providing altogether twelve theoretical cross sections per PDF that can be used to individually extract $\alpha_S(m_Z)$.

The PDF uncertainties of the theoretical fiducial cross sections are obtained by taking into account the different eigenvector sets, or replicas, that come with each of the PDFs. We use the "official" prescriptions of each PDF set to compute their associated uncertainties. More specifically, the PDF uncertainties are calculated from the cross sections obtained with the central PDF member (σ_0) and with the rest of eigenvalues or replicas (σ_i) as follows:

- For CT14, the uncertainty eigenvectors are considered in pairs from the $i = 1$–56 PDF members. The largest positive and negative differences from each pair are summed quadratically to obtain the corresponding positive and negative PDF uncertainties:

$$\Delta\sigma_\pm = \sqrt{\sum_{j=1}^{28} \max\left(\pm(\sigma_{2j-1} - \sigma_0),\, \pm(\sigma_{2j} - \sigma_0),\, 0\right)^2}.$$

  The CT14 PDF set results in asymmetric uncertainties interpreted as a 90% confidence level interval. To convert those to one standard deviation, as for the rest of PDF sets, they are divided by a factor of $\sqrt{2}\,\text{erf}^{-1}(0.9) \approx 1.645$.

- For HERAPDF2.0, a first asymmetric uncertainty is derived from the so-called 'EIG' (experimental uncertainties) PDF members, and a second one from the $i = 1$–10 'VAR' (variation) members, as for CT14. A third asymmetric uncertainty is taken from the $i = 11$–13 VAR members, as the maximum positive and negative differences $\Delta\sigma_i$ with respect to σ_0. Finally, all positive and negative uncertainties are separately added quadratically to get the final uncertainties.

JHEP06(2020)018

- For MMHT14, uncertainties are obtained from its corresponding 50 eigenvalues as done for CT14.

- For NNPDF3.0, the average cross section $\hat{\sigma}$ from replica members $i = 1$–100 is calculated first, and the associated standard deviation, $\sqrt{\sum_{i=1}^{100}(\sigma_i - \hat{\sigma})^2/99}$, is taken as the symmetric PDF uncertainty.

To determine the scale uncertainty associated with missing corrections beyond the NNLO accuracy, the MCFM cross sections are recalculated for each PDF and measurement using factorisation and renormalisation scales varied within factors of two, such that the ratio of the two scales is not less than 0.5 or more than 2. This gives seven combinations: (μ_F, μ_R), $(\mu_F/2, \mu_R/2)$, $(\mu_F/2, \mu_R)$, $(\mu_F, \mu_R/2)$, $(2\mu_F, \mu_R)$, $(\mu_F, 2\mu_R)$, $(2\mu_F, 2\mu_R)$. The largest and smallest cross sections of the seven combinations are determined, and the scale uncertainty is taken as half the difference of the extremal values. The scale variation uncertainties amount to 0.5–1% of the theoretical cross sections.

Since MCFM does not include EW corrections, arising from additional $W^{\pm}$, Z, and/or photons exchanged and/or radiated in the partonic process, those are computed separately. For this purpose, the MCSANC v.1.01 code [17] is used. For $e^{\pm}$ final states, we follow the "calorimetric" prescription, proposed in theoretical $W^{\pm}$ and Z boson production cross section benchmarking studies at the LHC [27], and recombine any radiated photon with the $e^{\pm}$ if their relative distance in the pseudorapidity-azimuth plane is $\Delta R = \sqrt{(\eta^e - \eta^\gamma)^2 + (\phi^e - \phi^\gamma)^2} < 0.1$. For $\mu^{\pm}$ final states, we use directly the "bare" MCSANC cross section. We run MCSANC at NLO with EW corrections on and off, and compute the corresponding multiplicative factor $K_{EW} = \sigma(\text{NLO,EW on})/\sigma(\text{NLO,EW off})$, which is used to correct the pQCD MCFM results. The EW corrections, in the range of 1–4%, are all negative, i.e. they reduce the overall cross section with respect to the pure pQCD result. Since the EW corrections are small, their associated uncertainties are neglected hereafter because they would propagate into the final computed $W^{\pm}$ and Z cross section at a few per mille level, below the numerical uncertainty of the MCFM calculation. Subtracting the EW corrections, rather than applying them multiplicatively via a K_{EW} factor as done here, gives consistent results within the (neglected) per mille uncertainties. For simplicity, in the MCSANC calculations, the electron pseudorapidity range $1.44 < |\eta| < 1.57$ (excluded in the actual measurements) is also included, since we are interested in the relative correction, this small range (present in both the numerator and denominator of the correcting factor) does not affect the K_{EW} ratio. The roles of photon-induced contributions and of mixed QCD⊕QED NLO corrections to Drell-Yan processes in pp collisions have been computed in refs. [28] and [29], respectively. The impact of such corrections to the inclusive $W^{\pm}$ and Z cross sections is at a few per mille level, and also neglected here.

All the relevant sources of uncertainties in the $W^{\pm}$ and Z boson cross sections are summarised in table 2. The largest experimental and theoretical uncertainties come from the integrated luminosity and PDF knowledge, respectively. Each calculated cross section has a numerical accuracy, as reported by MCFM, in the range of 0.2–0.6%. Such an uncertainty is commensurate with the typical differences encountered when computing NNLO $W^{\pm}$ and

JHEP06(2020)018

Uncertainties		Degree of correlation
Experimental:		
Integrated luminosity	2–4%	fully correlated at a given c.m. energy
Systematic	1–3%	partially correlated
Statistical	0.5–2%	uncorrelated
Theoretical:		
PDF	1–4%	partially correlated within each PDF set
Theoretical scale	0.3–1.3%	partially correlated
MCFM statistical numerical	0.2–0.6%	uncorrelated

Table 2. Summary of the typical experimental and theoretical uncertainties in the $W^{\pm}$ and Z boson production cross sections, and their degree of correlation (details are provided in section 5.3).

Z boson cross sections with different pQCD codes that implement higher-order virtual-real corrections with various methods [27].

4 EW boson fiducial cross sections: data versus theory

All the experimental and theoretical fiducial cross sections for W^+, W^-, and Z production in pp collisions are given in tables 3 and 4 for 7 and 8 TeV, respectively. For each measurement, the fiducial cross section definition and the experimental result are listed along with their uncertainties from the different sources listed in table 2. The theoretical MCFM predictions computed with all four PDF sets for their preferred default $\alpha_S(m_Z) = 0.118$ value are listed including their associated PDF, α_S (obtained, as described in section 5.2, from the cross section change when $\alpha_S(m_Z)$ is modified by ± 0.001), and scale uncertainties. For each system, the NLO MCSANC EW correction factors (absolute and relative) are also listed. For the results at $\sqrt{s} = 8$ TeV, the theoretical result obtained with the alternative FEWZ NNLO pQCD calculator [30], using the MSTW2008 PDF set [31] as provided in the original ref. [14], is also listed to show the very similar theoretical predictions expected with an alternative NNLO code and a pre-LHC PDF set.

For each of the twelve experimental $W^{\pm}$ and Z boson cross section measurements listed in table 1, we have computed their corresponding theoretical NNLO pQCD predictions using the four PDF sets and five to seven different values of $\alpha_S(m_Z)$. It is important to stress again that, for each QCD coupling constant, we use the specific PDF sets that are associated with that particular $\alpha_S(m_Z)$ value. We calculated the NLO EW corrections using NNPDF3.0 and $\alpha_S(m_Z) = 0.118$. By comparing the whole set of theoretical calculations to the experimental data, a preferred value of the QCD coupling constant can be derived for each PDF set as explained in the next section. Figures 1–2 show the fiducial cross sections as a function of $\alpha_S(m_Z)$, with the experimental values indicated by the horizontal black line with the inner grey band showing the integrated luminosity uncertainty, and the outer darker band showing the total experimental uncertainties added in quadrature. The filled

JHEP06(2020)018

System	Fiducial cross section
$pp \to W^+(e^+\nu) + X$, $\sqrt{s} = 7\,\text{TeV}$ ($p_T^e > 25\,\text{GeV}$, $\lvert\eta^e\rvert < 2.5$)	
Measurement [13]	$3404 \pm 12\,(\text{stat}) \pm 67\,(\text{syst}) \pm 136\,(\text{lumi})\,\text{pb}$
MCFM (NNLO, CT14)	$3361\,^{+93}_{-94}\,(\text{PDF}) \pm 30\,(\alpha_S) \pm 49\,(\text{scale}) \pm 18\,(\text{stat})\,\text{pb}$
MCFM (NNLO, HERAPDF2.0)	$3574\,^{+63}_{-94}\,(\text{PDF}) \pm 19\,(\alpha_S) \pm 33\,(\text{scale}) \pm 23\,(\text{stat})\,\text{pb}$
MCFM (NNLO, MMHT14)	$3407\,^{+92}_{-74}\,(\text{PDF}) \pm 37\,(\alpha_S) \pm 31\,(\text{scale}) \pm 18\,(\text{stat})\,\text{pb}$
MCFM (NNLO, NNPDF3.0)	$3345 \pm 70\,(\text{PDF}) \pm 32\,(\alpha_S) \pm 29\,(\text{scale}) \pm 18\,(\text{stat})\,\text{pb}$
MCSANC (NLO EW correction, NNPDF3.0)	$-36\,\text{pb}\ (-1.1\%)$
$pp \to W^-(e^-\overline{\nu}) + X$, $\sqrt{s} = 7\,\text{TeV}$ ($p_T^e > 25\,\text{GeV}$, $\lvert\eta^e\rvert < 2.5$)	
Measurement [13]	$2284 \pm 10\,(\text{stat}) \pm 43\,(\text{syst}) \pm 91\,(\text{lumi})\,\text{pb}$
MCFM (NNLO, CT14)	$2235\,^{+66}_{-57}\,(\text{PDF}) \pm 19\,(\alpha_S) \pm 19\,(\text{scale}) \pm 7\,(\text{stat})\,\text{pb}$
MCFM (NNLO, HERAPDF2.0)	$2319\,^{+21}_{-51}\,(\text{PDF}) \pm 8\,(\alpha_S) \pm 19\,(\text{scale}) \pm 7\,(\text{stat})\,\text{pb}$
MCFM (NNLO, MMHT14)	$2248\,^{+28}_{-62}\,(\text{PDF}) \pm 23\,(\alpha_S) \pm 17\,(\text{scale}) \pm 7\,(\text{stat})\,\text{pb}$
MCFM (NNLO, NNPDF3.0)	$2192 \pm 47\,(\text{PDF}) \pm 16\,(\alpha_S) \pm 16\,(\text{scale}) \pm 7\,(\text{stat})\,\text{pb}$
MCSANC (NLO EW correction, NNPDF3.0)	$-24\,\text{pb}\ (-1.1\%)$
$pp \to Z(e^+e^-) + X$, $\sqrt{s} = 7\,\text{TeV}$ ($p_T^e > 25\,\text{GeV}$, $\lvert\eta^e\rvert < 2.5$, $60 < m_Z < 120\,\text{GeV}$)	
Measurement [13]	$452 \pm 5\,(\text{stat}) \pm 10\,(\text{syst}) \pm 18\,(\text{lumi})\,\text{pb}$
MCFM (NNLO, CT14)	$430\,^{+11}_{-13}\,(\text{PDF}) \pm 4\,(\alpha_S) \pm 2\,(\text{scale}) \pm 1\,(\text{stat})\,\text{pb}$
MCFM (NNLO, HERAPDF2.0)	$444\,^{+4}_{-12}\,(\text{PDF}) \pm 2\,(\alpha_S) \pm 2\,(\text{scale}) \pm 1\,(\text{stat})\,\text{pb}$
MCFM (NNLO, MMHT14)	$433\,^{+6}_{-10}\,(\text{PDF}) \pm 5\,(\alpha_S) \pm 3\,(\text{scale}) \pm 1\,(\text{stat})\,\text{pb}$
MCFM (NNLO, NNPDF3.0)	$421 \pm 9\,(\text{PDF}) \pm 3\,(\alpha_S) \pm 2\,(\text{scale}) \pm 1\,(\text{stat})\,\text{pb}$
MCSANC (NLO EW correction, NNPDF3.0)	$-12\,\text{pb}\ (-2.6\%)$
$pp \to W^+(\mu^+\nu) + X$, $\sqrt{s} = 7\,\text{TeV}$ ($p_T^\mu > 25\,\text{GeV}$, $\lvert\eta^\mu\rvert < 2.1$)	
Measurement [13]	$2815 \pm 9\,(\text{stat}) \pm 42\,(\text{syst}) \pm 113\,(\text{lumi})\,\text{pb}$
MCFM (NNLO, CT14)	$2827\,^{+65}_{-110}\,(\text{PDF}) \pm 29\,(\alpha_S) \pm 21\,(\text{scale}) \pm 13\,(\text{stat})\,\text{pb}$
MCFM (NNLO, HERAPDF2.0)	$2976\,^{+42}_{-118}\,(\text{PDF}) \pm 16\,(\alpha_S) \pm 37\,(\text{scale}) \pm 15\,(\text{stat})\,\text{pb}$
MCFM (NNLO, MMHT14)	$2833\,^{+63}_{-90}\,(\text{PDF}) \pm 29\,(\alpha_S) \pm 17\,(\text{scale}) \pm 16\,(\text{stat})\,\text{pb}$
MCFM (NNLO, NNPDF3.0)	$2806 \pm 62\,(\text{PDF}) \pm 26\,(\alpha_S) \pm 29\,(\text{scale}) \pm 15\,(\text{stat})\,\text{pb}$
MCSANC (NLO EW correction, NNPDF3.0)	$-64\,\text{pb}\ (-2.2\%)$
$pp \to W^-(\mu^-\overline{\nu}) + X$, $\sqrt{s} = 7\,\text{TeV}$ ($p_T^\mu > 25\,\text{GeV}$, $\lvert\eta^\mu\rvert < 2.1$)	
Measurement [13]	$1921 \pm 8\,(\text{stat}) \pm 27\,(\text{syst}) \pm 77\,(\text{lumi})\,\text{pb}$
MCFM (NNLO, CT14)	$1915\,^{+43}_{-68}\,(\text{PDF}) \pm 19\,(\alpha_S) \pm 16\,(\text{scale}) \pm 6\,(\text{stat})\,\text{pb}$
MCFM (NNLO, HERAPDF2.0)	$1976\,^{+33}_{-29}\,(\text{PDF}) \pm 8\,(\alpha_S) \pm 19\,(\text{scale}) \pm 6\,(\text{stat})\,\text{pb}$
MCFM (NNLO, MMHT14)	$1937\,^{+33}_{-41}\,(\text{PDF}) \pm 20\,(\alpha_S) \pm 17\,(\text{scale}) \pm 6\,(\text{stat})\,\text{pb}$
MCFM (NNLO, NNPDF3.0)	$1877 \pm 40\,(\text{PDF}) \pm 13\,(\alpha_S) \pm 17\,(\text{scale}) \pm 6\,(\text{stat})\,\text{pb}$
MCSANC (NLO EW correction, NNPDF3.0)	$-42\,\text{pb}\ (-2.2\%)$
$pp \to Z(\mu^+\mu^-) + X$, $\sqrt{s} = 7\,\text{TeV}$ ($p_T^\mu > 20\,\text{GeV}$, $\lvert\eta^\mu\rvert < 2.1$, $60 < m_Z < 120\,\text{GeV}$)	
Measurement [13]	$396 \pm 3\,(\text{stat}) \pm 7\,(\text{syst}) \pm 16\,(\text{lumi})\,\text{pb}$
MCFM (NNLO, CT14)	$380\,^{+7}_{-16}\,(\text{PDF}) \pm 3\,(\alpha_S) \pm 2\,(\text{scale}) \pm 1\,(\text{stat})\,\text{pb}$
MCFM (NNLO, HERAPDF2.0)	$392\,^{+6}_{-6}\,(\text{PDF}) \pm 2\,(\alpha_S) \pm 2\,(\text{scale}) \pm 1\,(\text{stat})\,\text{pb}$
MCFM (NNLO, MMHT14)	$382\,^{+11}_{-4}\,(\text{PDF}) \pm 4\,(\alpha_S) \pm 2\,(\text{scale}) \pm 1\,(\text{stat})\,\text{pb}$
MCFM (NNLO, NNPDF3.0)	$373 \pm 8\,(\text{PDF}) \pm 3\,(\alpha_S) \pm 2\,(\text{scale}) \pm 1\,(\text{stat})\,\text{pb}$
MCSANC (NLO EW correction, NNPDF3.0)	$-14\,\text{pb}\ (-3.9\%)$

Table 3. Experimental and theoretical fiducial cross sections for $W^\pm$ and Z production in pp collisions at $\sqrt{s} = 7\,\text{TeV}$, with the uncertainty sources listed in table 2. The NNLO pQCD results are obtained with MCFM for $\alpha_S(m_Z) = 0.118$ using the CT14, HERAPDF2.0, MMHT14, and NNPDF3.0 PDF sets. (The quoted α_S uncertainties are derived from the cross section changes when $\alpha_S(m_Z)$ is modified by ± 0.001). The NLO EW corrections are computed with MCSANC.

ellipses represent the contours of the joint probability density functions (Jpdfs) of the theoretical and experimental results, with a width representing a two-dimensional one standard deviation obtained from the product of the probability densities of the experimental and

JHEP06(2020)018

System	Fiducial cross section
$pp \to W^+(e^+\nu) + X$, $\sqrt{s} = 8\,\text{TeV}$ ($p_T^e > 25\,\text{GeV}$, $\lvert\eta^e\rvert < 1.44$, $1.57 < \lvert\eta^e\rvert < 2.5$)	
Measurement [14]	$3540 \pm 20\,(\text{stat}) \pm 110\,(\text{syst}) \pm 90\,(\text{lumi})\,\text{pb}$
FEWZ (NNLO, MSTW2008) [14]	$3450 \pm 120\,\text{pb}$
MCFM (NNLO, CT14)	$3522\,^{+113}_{-123}\,(\text{PDF}) \pm 23\,(\alpha_S) \pm 35\,(\text{scale}) \pm 21\,(\text{stat})\,\text{pb}$
MCFM (NNLO, HERAPDF2.0)	$3721\,^{+127}_{-97}\,(\text{PDF}) \pm 13\,(\alpha_S) \pm 48\,(\text{scale}) \pm 22\,(\text{stat})\,\text{pb}$
MCFM (NNLO, MMHT14)	$3581\,^{+61}_{-137}\,(\text{PDF}) \pm 36\,(\alpha_S) \pm 38\,(\text{scale}) \pm 20\,(\text{stat})\,\text{pb}$
MCFM (NNLO, NNPDF3.0)	$3515 \pm 75\,(\text{PDF}) \pm 34\,(\alpha_S) \pm 42\,(\text{scale}) \pm 20\,(\text{stat})\,\text{pb}$
MCSANC (NLO EW correction, NNPDF3.0)	$-45\,\text{pb}\ (-1.2\%)$
$pp \to W^-(e^-\overline{\nu}) + X$, $\sqrt{s} = 8\,\text{TeV}$ ($p_T^e > 25\,\text{GeV}$, $\lvert\eta^e\rvert < 1.44$, $1.57 < \lvert\eta^e\rvert < 2.5$)	
Measurement [14]	$2390 \pm 10\,(\text{stat}) \pm 60\,(\text{syst}) \pm 60\,(\text{lumi})\,\text{pb}$
FEWZ (NNLO, MSTW2008) [14]	$2380 \pm 90\,\text{pb}$
MCFM (NNLO, CT14)	$2426\,^{+69}_{-61}\,(\text{PDF}) \pm 24\,(\alpha_S) \pm 14\,(\text{scale}) \pm 8\,(\text{stat})\,\text{pb}$
MCFM (NNLO, HERAPDF2.0)	$2513\,^{+51}_{-44}\,(\text{PDF}) \pm 11\,(\alpha_S) \pm 21\,(\text{scale}) \pm 10\,(\text{stat})\,\text{pb}$
MCFM (NNLO, MMHT14)	$2445\,^{+40}_{-67}\,(\text{PDF}) \pm 28\,(\alpha_S) \pm 26\,(\text{scale}) \pm 8\,(\text{stat})\,\text{pb}$
MCFM (NNLO, NNPDF3.0)	$2375 \pm 51\,(\text{PDF}) \pm 17\,(\alpha_S) \pm 14\,(\text{scale}) \pm 8\,(\text{stat})\,\text{pb}$
MCSANC (NLO EW correction, NNPDF3.0)	$-30\,\text{pb}\ (-1.2\%)$
$pp \to Z(e^+e^-) + X$, $\sqrt{s} = 8\,\text{TeV}$ ($p_T^e > 25\,\text{GeV}$, $\lvert\eta^e\rvert < 1.44$, $1.57 < \lvert\eta^e\rvert < 2.5$, $60 < m_Z < 120\,\text{GeV}$)	
Measurement [14]	$450 \pm 10\,(\text{stat}) \pm 10\,(\text{syst}) \pm 10\,(\text{lumi})\,\text{pb}$
FEWZ (NNLO, MSTW2008) [14]	$450 \pm 20\,\text{pb}$
MCFM (NNLO, CT14)	$437\,^{+11}_{-15}\,(\text{PDF}) \pm 4\,(\alpha_S) \pm 2\,(\text{scale}) \pm 1\,(\text{stat})\,\text{pb}$
MCFM (NNLO, HERAPDF2.0)	$451\,^{+7}_{-11}\,(\text{PDF}) \pm 2\,(\alpha_S) \pm 2\,(\text{scale}) \pm 1\,(\text{stat})\,\text{pb}$
MCFM (NNLO, MMHT14)	$441\,^{+11}_{-6}\,(\text{PDF}) \pm 5\,(\alpha_S) \pm 3\,(\text{scale}) \pm 1\,(\text{stat})\,\text{pb}$
MCFM (NNLO, NNPDF3.0)	$429 \pm 9\,(\text{PDF}) \pm 3\,(\alpha_S) \pm 2\,(\text{scale}) \pm 1\,(\text{stat})\,\text{pb}$
MCSANC (NLO EW correction, NNPDF3.0)	$-13\,\text{pb}\ (-2.7\%)$
$pp \to W^+(\mu^+\nu) + X$, $\sqrt{s} = 8\,\text{TeV}$ ($p_T^\mu > 25\,\text{GeV}$, $\lvert\eta^\mu\rvert < 2.1$)	
Measurement [14]	$3100 \pm 10\,(\text{stat}) \pm 40\,(\text{syst}) \pm 80\,(\text{lumi})\,\text{pb}$
FEWZ (NNLO, MSTW2008) [14]	$3140 \pm 110\,\text{pb}$
MCFM (NNLO, CT14)	$3108\,^{+94}_{-87}\,(\text{PDF}) \pm 25\,(\alpha_S) \pm 34\,(\text{scale}) \pm 19\,(\text{stat})\,\text{pb}$
MCFM (NNLO, HERAPDF2.0)	$3309\,^{+20}_{-153}\,(\text{PDF}) \pm 18\,(\alpha_S) \pm 34\,(\text{scale}) \pm 17\,(\text{stat})\,\text{pb}$
MCFM (NNLO, MMHT14)	$3148\,^{+67}_{-95}\,(\text{PDF}) \pm 33\,(\alpha_S) \pm 29\,(\text{scale}) \pm 15\,(\text{stat})\,\text{pb}$
MCFM (NNLO, NNPDF3.0)	$3095 \pm 69\,(\text{PDF}) \pm 30\,(\alpha_S) \pm 21\,(\text{scale}) \pm 18\,(\text{stat})\,\text{pb}$
MCSANC (NLO EW correction, NNPDF3.0)	$-77\,\text{pb}\ (-2.4\%)$
$pp \to W^-(\mu^-\overline{\nu}) + X$, $\sqrt{s} = 8\,\text{TeV}$ ($p_T^\mu > 25\,\text{GeV}$, $\lvert\eta^\mu\rvert < 2.1$)	
Measurement [14]	$2240 \pm 10\,(\text{stat}) \pm 20\,(\text{syst}) \pm 60\,(\text{lumi})\,\text{pb}$
FEWZ (NNLO, MSTW2008) [14]	$2220 \pm 80\,\text{pb}$
MCFM (NNLO, CT14)	$2187\,^{+74}_{-56}\,(\text{PDF}) \pm 19\,(\alpha_S) \pm 14\,(\text{scale}) \pm 6\,(\text{stat})\,\text{pb}$
MCFM (NNLO, HERAPDF2.0)	$2274\,^{+40}_{-20}\,(\text{PDF}) \pm 10\,(\alpha_S) \pm 17\,(\text{scale}) \pm 7\,(\text{stat})\,\text{pb}$
MCFM (NNLO, MMHT14)	$2200\,^{+42}_{-36}\,(\text{PDF}) \pm 23\,(\alpha_S) \pm 20\,(\text{scale}) \pm 7\,(\text{stat})\,\text{pb}$
MCFM (NNLO, NNPDF3.0)	$2148 \pm 48\,(\text{PDF}) \pm 16\,(\alpha_S) \pm 17\,(\text{scale}) \pm 7\,(\text{stat})\,\text{pb}$
MCSANC (NLO EW correction, NNPDF3.0)	$-47\,\text{pb}\ (-2.1\%)$
$pp \to Z(\mu^+\mu^-) + X$, $\sqrt{s} = 8\,\text{TeV}$ ($p_T^\mu > 25\,\text{GeV}$, $\lvert\eta^\mu\rvert < 2.1$, $60 < m_Z < 120\,\text{GeV}$)	
Measurement [14]	$400 \pm 10\,(\text{stat}) \pm 10\,(\text{syst}) \pm 10\,(\text{lumi})\,\text{pb}$
FEWZ (NNLO, MSTW2008) [14]	$400 \pm 10\,\text{pb}$
MCFM (NNLO, CT14)	$389\,^{+12}_{-12}\,(\text{PDF}) \pm 3\,(\alpha_S) \pm 2\,(\text{scale}) \pm 1\,(\text{stat})\,\text{pb}$
MCFM (NNLO, HERAPDF2.0)	$401\,^{+6}_{-8}\,(\text{PDF}) \pm 2\,(\alpha_S) \pm 2\,(\text{scale}) \pm 1\,(\text{stat})\,\text{pb}$
MCFM (NNLO, MMHT14)	$391\,^{+11}_{-3}\,(\text{PDF}) \pm 4\,(\alpha_S) \pm 2\,(\text{scale}) \pm 1\,(\text{stat})\,\text{pb}$
MCFM (NNLO, NNPDF3.0)	$381 \pm 8\,(\text{PDF}) \pm 3\,(\alpha_S) \pm 2\,(\text{scale}) \pm 1\,(\text{stat})\,\text{pb}$
MCSANC (NLO EW correction, NNPDF3.0)	$-16\,\text{pb}\ (-3.9\%)$

Table 4. Experimental and theoretical fiducial cross sections for $W^\pm$ and Z production in pp collisions at $\sqrt{s} = 8\,\text{TeV}$, with the uncertainty sources listed in table 2. The NNLO pQCD results are obtained with MCFM for $\alpha_S(m_Z) = 0.118$ using the CT14, HERAPDF2.0, MMHT14, and NNPDF3.0 PDF sets, as well as with FEWZ using the MSTW2008 PDF. (The quoted α_S uncertainties are derived from the cross section changes when $\alpha_S(m_Z)$ is modified by ± 0.001). The NLO EW corrections are computed with MCSANC.

JHEP06(2020)018

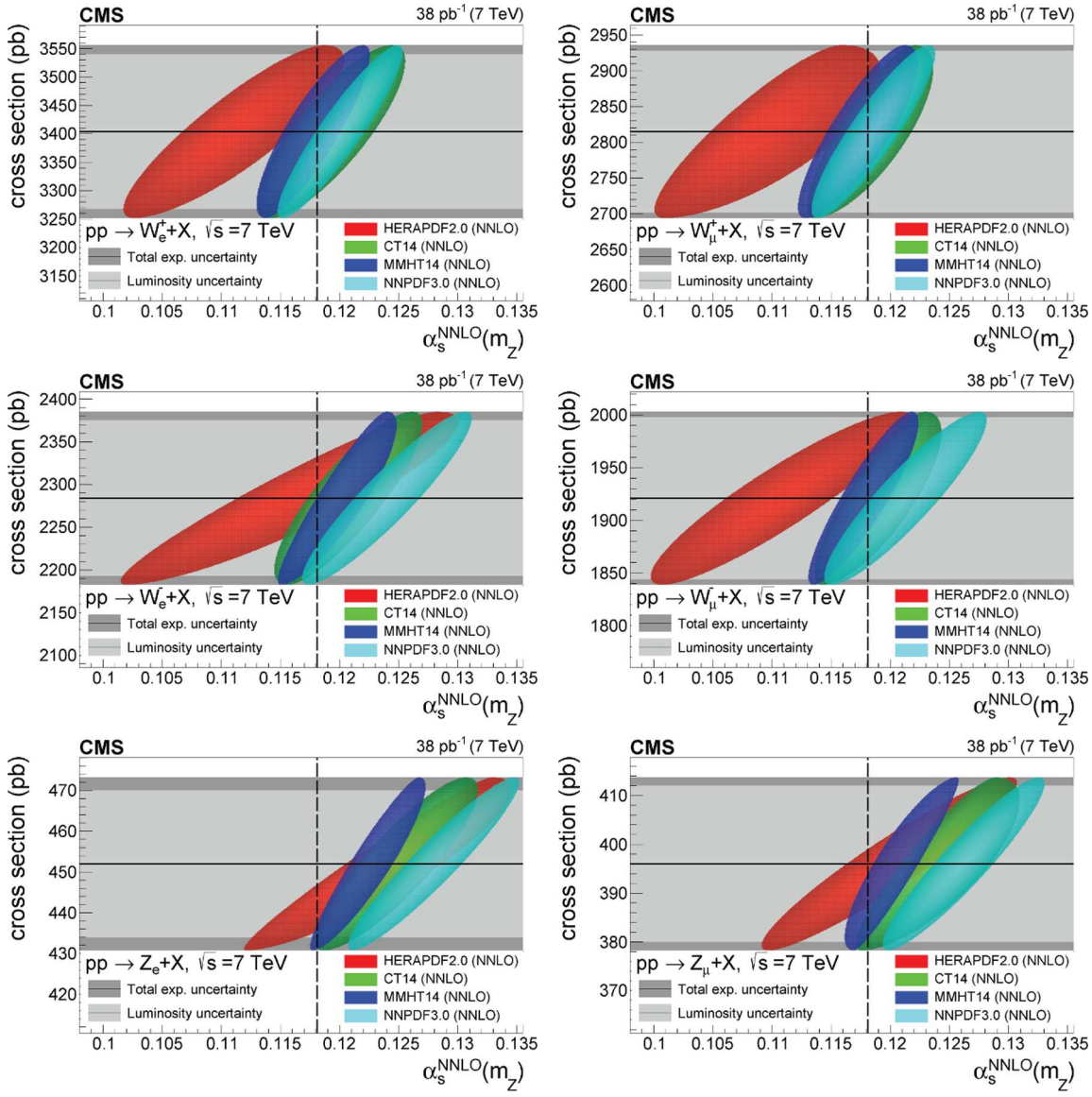

Figure 1. Experimental fiducial cross section for the production of W_e^+ (upper left) and W_μ^+ (upper right), W_e^- (middle left) and W_μ^- (middle right), and Z_e (lower left) and Z_μ (lower right) in pp collisions at $\sqrt{s} = 7\,\text{TeV}$ compared to the corresponding joint probability density functions (elliptical contours, see text) obtained with four different PDFs as a function of $\alpha_S(m_Z)$ and σ. The experimental measurements are plotted as a horizontal black line with the inner grey band indicating the integrated luminosity uncertainty, and the outer darker band showing all experimental uncertainties added in quadrature. The filled ellipses are obtained from the product of the probability distributions of the experimental and theoretical results for each PDF, and represent the two-dimensional one standard deviation. The points where the filled ellipses cross the vertical dashed line at $\alpha_S(m_Z) = 0.118$ indicate the most likely cross section interval that would be obtained using the baseline QCD coupling constant value of all PDF sets.

theoretical results for each PDF, as described in the next section. For any fixed value of $\alpha_S(m_Z)$, a hierarchy of $W^\pm$, Z theoretical cross sections is apparent with HERAPDF2.0

JHEP06(2020)018

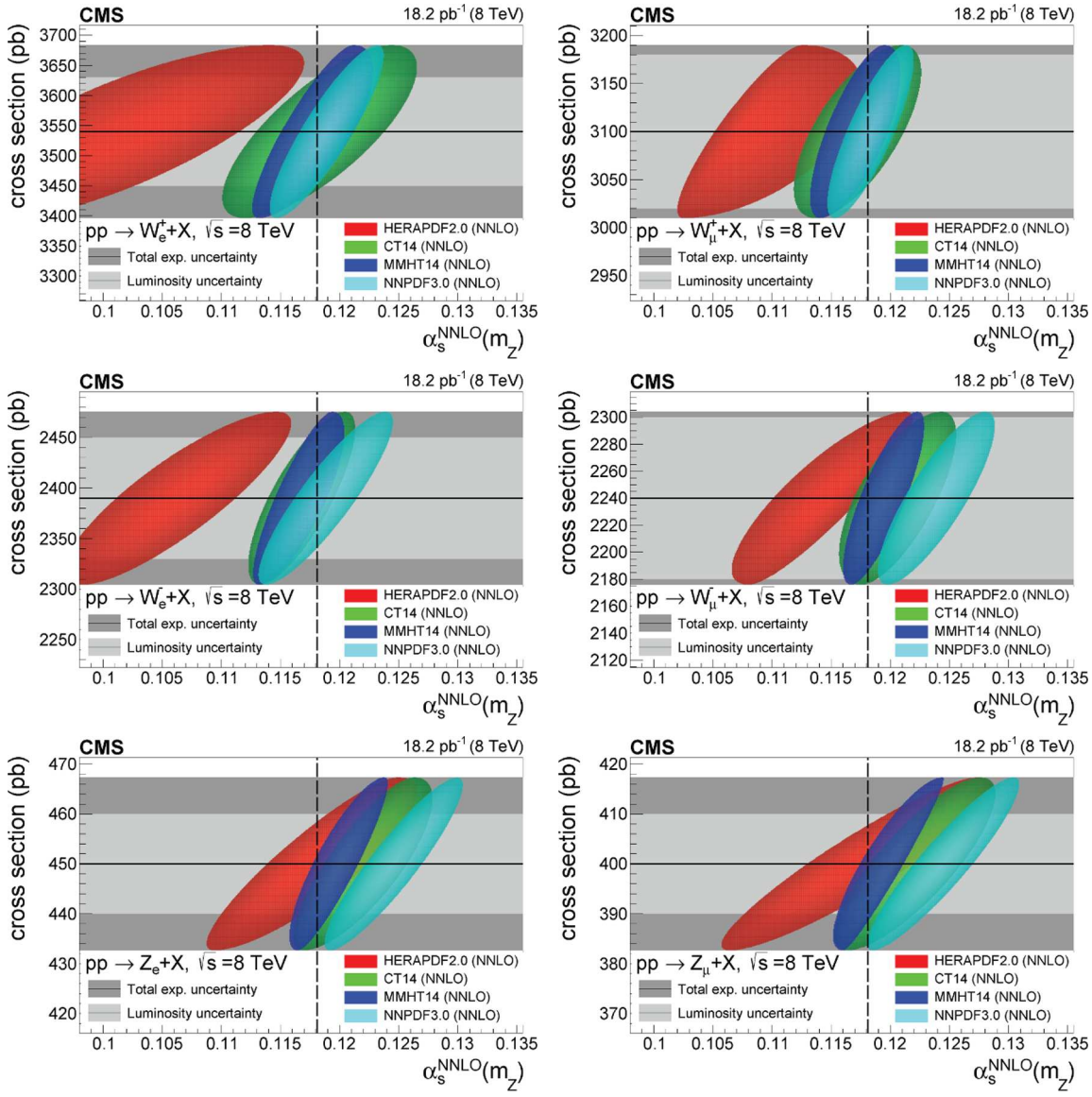

Figure 2. Same as figure 1 for the production of W_e^+ (upper left) and W_μ^+ (upper right), W_e^- (middle left) and W_μ^- (middle right), and Z_e (lower left) and Z_μ (lower right) in pp collisions at $\sqrt{s} = 8\,\text{TeV}$.

predictions tending to be systematically above the data, and the NNPDF3.0 ones below the latter. In between the results of these two PDF sets, the cross sections derived with MMHT14 tend to be above those with CT14, although they are often very similar and overlap most of the time. Alternatively, the results of figures 1–2 indicate that, in order to reproduce the experimental cross sections, HERAPDF2.0 (NNPDF3.0) tends in general to prefer a smaller (larger) value of $\alpha_S(m_Z)$ than other PDFs, and that the predictions from CT14 and MMHT14 tend to be less scattered over the $\alpha_S(m_Z)$ axis than those from HERAPDF2.0 and NNPDF3.0. The HERAPDF2.0 (MMHT14) filled ellipses have the smallest (largest) relative slope as a function of $\alpha_S(m_Z)$. A larger slope is advantageous for

JHEP06(2020)018

	CT14	HERAPDF2.0	MMHT14	NNPDF3.0
χ^2/ndf (symmetrised to the largest PDF uncertainty value)	12.0/11	11.0/11	9.0/11	31.7/11
χ^2/ndf (symmetrised to the smallest PDF uncertainty value)	15.2/11	28.3/11	13.9/11	31.7/11

Table 5. Overall goodness-of-fit per number of degrees of freedom, χ^2/ndf, among the twelve experimental measurements of $\mathrm{W}^{\pm}$ and Z boson production cross sections and the corresponding theoretical calculations obtained with the four different PDF sets for their default $\alpha_{\mathrm{S}}(m_{\mathrm{Z}}) = 0.118$ value. The first (second) row is obtained symmetrising the PDF uncertainties of the cross sections obtained with the CT14, HERAPDF2.0, and MMHT14 sets to the largest (smallest) of their respective values.

extracting the strong coupling constant, because this means that the underlying $\alpha_{\mathrm{S}}(m_{\mathrm{Z}})$ value in the calculations has a larger impact on the computed cross sections, also leading to a lower propagated uncertainty in the $\alpha_{\mathrm{S}}(m_{\mathrm{Z}})$ value derived by comparing the theoretical prediction to the experimental value.

Overall, the theoretical predictions computed using the world-average value of the QCD coupling constant (vertical dashed line in figures 1–2) agree well with the experimental values within the uncertainties. The level of data-theory agreement can be quantified with a goodness-of-fit test, $\chi^2 = \xi_i (M^{-1})_{ij} \xi_j$, where M is the covariance matrix taking all the uncertainties and their correlations into account, as explained in section 5.3, and $\xi_i = \sigma_{i,\mathrm{th}} - \sigma_{i,\mathrm{exp}}$ is the difference between theoretical and experimental cross sections for each PDF set. In the χ^2 calculation, the asymmetric uncertainties of the CT14, HERAPDF2.0, and MMHT14 PDF sets are symmetrised to the largest of the two values and also separately to the smallest of the two values. The results are listed in table 5.

5 Extraction of the QCD coupling constant

5.1 Extraction of $\alpha_{\mathrm{S}}(m_{\mathrm{Z}})$ for each single $\mathrm{W}^{\pm}$ and Z cross section measurement

The dependence of the theoretical cross sections on the QCD coupling constant $\alpha_{\mathrm{S}}(m_{\mathrm{Z}})$, shown in figures 1–2, is fitted through a linear χ^2-minimisation procedure over $\alpha_{\mathrm{S}}(m_{\mathrm{Z}}) \in [0.115, 0.121]$, to extract the slope k. Over the considered $\alpha_{\mathrm{S}}(m_{\mathrm{Z}})$ range, the empirical linear fit describes well the observed α_{S}-dependence of the theoretical cross section for all PDF sets. The value of $\alpha_{\mathrm{S}}(m_{\mathrm{Z}})$ preferred by each individual measurement is determined by the crossing point of the fitted linear theoretical curve with the experimental horizontal line. The resulting $\alpha_{\mathrm{S}}(m_{\mathrm{Z}})$ values are listed in table 6. For each theoretical point used in the fit, the uncertainty in the cross section is given by the quadratic sum of its associated PDF, scale, and numerical uncertainties. In order to exploit the dependence of $\sigma_{\mathrm{th}}(\mathrm{V})$ on α_{S} to quantitatively derive the latter, a joint probability density function is constructed for each PDF prediction, as explained next. When the theoretical cross section value has positive and negative uncertainties $\delta_{+\text{-}}$, the experimental cross section is σ_{exp} with uncertainty δ_{exp}, the slope of the fit is k, and the fitted QCD coupling constant is $\alpha_{\mathrm{S}}(m_{\mathrm{Z}})$, then the Jpdf as a function of σ and α_{S} is proportional to

$$\exp\left\{-\frac{1}{2}\left[\left(\frac{\sigma-\sigma_{\mathrm{exp}}}{\delta_{\mathrm{exp}}}\right)^2+\left(\frac{\sigma-\sigma_{\mathrm{exp}}-k(\alpha_{\mathrm{S}}-\alpha_{\mathrm{S}}(m_{\mathrm{Z}}))}{\delta_{+\text{-}}}\right)^2\right]\right\}. \tag{5.1}$$

JHEP06(2020)018

Cross section	PDF	$\alpha_S(m_Z)$ (total)	δ_{α_S} (stat)	δ_{α_S} (lumi)	δ_{α_S} (syst)	δ_{α_S}(PDF)	δ_{α_S}(scale)	δ_{α_S} (num)
W_e^+ (7 TeV)	CT14	$0.1193\ ^{+0.0062}_{-0.0062}$	0.0004	0.0046	0.0022	$^{+0.0031}_{-0.0032}$	0.0017	0.0006
	HERAPDF2.0	$0.1108\ ^{+0.0090}_{-0.0097}$	0.0006	0.0072	0.0035	$^{+0.0033}_{-0.0050}$	0.0017	0.0012
	MMHT14	$0.1179\ ^{+0.0049}_{-0.0047}$	0.0003	0.0037	0.0018	$^{+0.0025}_{-0.0020}$	0.0008	0.0005
	NNPDF3.0	$0.1200\ ^{+0.0054}_{-0.0054}$	0.0004	0.0043	0.0021	$^{+0.0022}_{-0.0022}$	0.0009	0.0006
W_e^- (7 TeV)	CT14	$0.1208\ ^{+0.0064}_{-0.0061}$	0.0005	0.0047	0.0022	$^{+0.0034}_{-0.0030}$	0.001	0.0004
	HERAPDF2.0	$0.1152\ ^{+0.0136}_{-0.0149}$	0.0013	0.0118	0.0056	$^{+0.0027}_{-0.0066}$	0.0025	0.0009
	MMHT14	$0.1195\ ^{+0.0047}_{-0.0053}$	0.0004	0.0040	0.0019	$^{+0.0012}_{-0.0027}$	0.0007	0.0003
	NNPDF3.0	$0.1239\ ^{+0.0073}_{-0.0073}$	0.0007	0.0060	0.0028	$^{+0.0029}_{-0.0029}$	0.0011	0.0005
Z_e (7 TeV)	CT14	$0.1247\ ^{+0.0068}_{-0.0070}$	0.0014	0.0051	0.0028	$^{+0.0031}_{-0.0036}$	0.0004	0.0003
	HERAPDF2.0	$0.1226\ ^{+0.0106}_{-0.0121}$	0.0025	0.0088	0.0049	$^{+0.0018}_{-0.0061}$	0.0007	0.0005
	MMHT14	$0.1222\ ^{+0.0047}_{-0.0050}$	0.0011	0.0038	0.0021	$^{+0.0012}_{-0.0022}$	0.0006	0.0002
	NNPDF3.0	$0.1279\ ^{+0.0074}_{-0.0074}$	0.0016	0.0058	0.0032	$^{+0.0027}_{-0.0027}$	0.0007	0.0003
W_μ^+ (7 TeV)	CT14	$0.1178\ ^{+0.0049}_{-0.0058}$	0.0003	0.0040	0.0015	$^{+0.0023}_{-0.0039}$	0.0007	0.0005
	HERAPDF2.0	$0.1085\ ^{+0.0083}_{-0.0108}$	0.0006	0.0070	0.0026	$^{+0.0026}_{-0.0073}$	0.0023	0.0009
	MMHT14	$0.1170\ ^{+0.0048}_{-0.0053}$	0.0003	0.0039	0.0015	$^{+0.0022}_{-0.0031}$	0.0006	0.0006
	NNPDF3.0	$0.1185\ ^{+0.0054}_{-0.0054}$	0.0003	0.0044	0.0016	$^{+0.0022}_{-0.0022}$	0.0011	0.0006
W_μ^- (7 TeV)	CT14	$0.1186\ ^{+0.0050}_{-0.0057}$	0.0004	0.0041	0.0014	$^{+0.0023}_{-0.0036}$	0.0009	0.0003
	HERAPDF2.0	$0.1109\ ^{+0.0111}_{-0.0109}$	0.001	0.0094	0.0033	$^{+0.0040}_{-0.0035}$	0.0023	0.0008
	MMHT14	$0.1177\ ^{+0.0046}_{-0.0047}$	0.0004	0.0039	0.0014	$^{+0.0017}_{-0.0021}$	0.0009	0.0003
	NNPDF3.0	$0.1212\ ^{+0.0070}_{-0.0070}$	0.0006	0.0058	0.0020	$^{+0.0029}_{-0.0029}$	0.0013	0.0004
Z_μ (7 TeV)	CT14	$0.1232\ ^{+0.0062}_{-0.0077}$	0.001	0.0051	0.0022	$^{+0.0023}_{-0.0051}$	0.0005	0.0003
	HERAPDF2.0	$0.1200\ ^{+0.0108}_{-0.0108}$	0.0017	0.0092	0.0040	$^{+0.0034}_{-0.0034}$	0.0012	0.0005
	MMHT14	$0.1213\ ^{+0.0051}_{-0.0045}$	0.0007	0.0039	0.0017	$^{+0.0027}_{-0.001}$	0.0005	0.0002
	NNPDF3.0	$0.1261\ ^{+0.0070}_{-0.0070}$	0.0011	0.0057	0.0025	$^{+0.0028}_{-0.0028}$	0.0007	0.0003
W_e^+ (8 TeV)	CT14	$0.1181\ ^{+0.0081}_{-0.0083}$	0.0009	0.0039	0.0047	$^{+0.0049}_{-0.0053}$	0.0015	0.0009
	HERAPDF2.0	$0.1030\ ^{+0.0154}_{-0.0140}$	0.0015	0.0070	0.0085	$^{+0.0099}_{-0.0075}$	0.0037	0.0017
	MMHT14	$0.1172\ ^{+0.0045}_{-0.0057}$	0.0006	0.0025	0.0031	$^{+0.0017}_{-0.0039}$	0.0011	0.0006
	NNPDF3.0	$0.1188\ ^{+0.0049}_{-0.0049}$	0.0006	0.0027	0.0032	$^{+0.0022}_{-0.0022}$	0.0012	0.0006
W_e^- (8 TeV)	CT14	$0.1169\ ^{+0.0046}_{-0.0044}$	0.0004	0.0025	0.0025	$^{+0.0029}_{-0.0025}$	0.0006	0.0003
	HERAPDF2.0	$0.1066\ ^{+0.0098}_{-0.0094}$	0.001	0.0057	0.0057	$^{+0.0049}_{-0.0042}$	0.0020	0.0009
	MMHT14	$0.1163\ ^{+0.0036}_{-0.0041}$	0.0004	0.0022	0.0022	$^{+0.0014}_{-0.0025}$	0.001	0.0003
	NNPDF3.0	$0.1187\ ^{+0.0059}_{-0.0059}$	0.0006	0.0035	0.0035	$^{+0.0029}_{-0.0029}$	0.0008	0.0005
Z_e (8 TeV)	CT14	$0.1216\ ^{+0.0056}_{-0.0062}$	0.0027	0.0027	0.0027	$^{+0.0029}_{-0.0040}$	0.0007	0.0003
	HERAPDF2.0	$0.1173\ ^{+0.0084}_{-0.0093}$	0.0045	0.0045	0.0045	$^{+0.0031}_{-0.0051}$	0.0009	0.0005
	MMHT14	$0.1201\ ^{+0.0044}_{-0.0039}$	0.0021	0.0021	0.0021	$^{+0.0023}_{-0.0013}$	0.0006	0.0002
	NNPDF3.0	$0.1245\ ^{+0.0060}_{-0.0060}$	0.0031	0.0031	0.0031	$^{+0.0027}_{-0.0027}$	0.0006	0.0003
W_μ^+ (8 TeV)	CT14	$0.1173\ ^{+0.0055}_{-0.0053}$	0.0004	0.0032	0.0016	$^{+0.0038}_{-0.0035}$	0.0014	0.0008
	HERAPDF2.0	$0.1076\ ^{+0.0055}_{-0.0101}$	0.0006	0.0045	0.0022	$^{+0.0011}_{-0.0085}$	0.0019	0.0009
	MMHT14	$0.1168\ ^{+0.0035}_{-0.0041}$	0.0003	0.0024	0.0012	$^{+0.0020}_{-0.0029}$	0.0009	0.0005
	NNPDF3.0	$0.1182\ ^{+0.0038}_{-0.0038}$	0.0003	0.0027	0.0013	$^{+0.0022}_{-0.0022}$	0.0007	0.0006
W_μ^- (8 TeV)	CT14	$0.1209\ ^{+0.0053}_{-0.0046}$	0.0005	0.0032	0.0011	$^{+0.0039}_{-0.0030}$	0.0008	0.0003
	HERAPDF2.0	$0.1147\ ^{+0.0081}_{-0.0072}$	0.0010	0.0062	0.0021	$^{+0.0041}_{-0.0021}$	0.0018	0.0007
	MMHT14	$0.1195\ ^{+0.0035}_{-0.0034}$	0.0004	0.0026	0.0009	$^{+0.0019}_{-0.0016}$	0.0009	0.0003
	NNPDF3.0	$0.1238\ ^{+0.0052}_{-0.0052}$	0.0006	0.0039	0.0013	$^{+0.0029}_{-0.0029}$	0.0011	0.0004
Z_μ (8 TeV)	CT14	$0.1220\ ^{+0.0067}_{-0.0069}$	0.0032	0.0032	0.0032	$^{+0.0037}_{-0.0040}$	0.0006	0.0003
	HERAPDF2.0	$0.1170\ ^{+0.0112}_{-0.0116}$	0.0060	0.0060	0.0060	$^{+0.0036}_{-0.0048}$	0.0013	0.0006
	MMHT14	$0.1202\ ^{+0.0050}_{-0.0043}$	0.0024	0.0024	0.0024	$^{+0.0027}_{-0.0007}$	0.0005	0.0002
	NNPDF3.0	$0.1244\ ^{+0.0066}_{-0.0066}$	0.0034	0.0034	0.0034	$^{+0.0028}_{-0.0028}$	0.0006	0.0003

Table 6. Extracted $\alpha_S(m_Z)$ values from the different data-theory $W^\pm$ and Z boson production cross section comparisons for each PDF set, with associated uncertainties from different experimental (statistical, integrated luminosity, and systematic) and theoretical (PDF, scale, and numerical) sources.

JHEP06(2020)018

The sign of $(\sigma - \sigma_{\rm exp} - k(\alpha_{\rm S} - \alpha_{\rm S}(m_{\rm Z})))$ determines which of the $\delta_{+\text{-}}$ is used. For symmetric uncertainties the Jpdfs have elliptical contours, but for asymmetric ones they are two filled ellipses combined together. This procedure is repeated for all the twelve different measurements and for all four PDF sets, and plotted as the filled ellipses shown in figures 1–2, where each coloured area corresponds to one two-dimensional (in σ and $\alpha_{\rm S}(m_{\rm Z})$) standard deviation.

5.2 Propagation of $\alpha_{\rm S}(m_{\rm Z})$ uncertainties

Appropriate propagation of the separated experimental and theoretical uncertainties into each value of $\alpha_{\rm S}(m_{\rm Z})$ obtained from each particular $\rm W^{\pm}$ and Z measurement, is crucial to combine all estimates taking into account their correlations, and extract a single final $\alpha_{\rm S}(m_{\rm Z})$ result. The method employed to determine the individual sources of uncertainties associated with a given $\alpha_{\rm S}(m_{\rm Z})$ value is similar to that used in refs. [8, 9] for the $\alpha_{\rm S}(m_{\rm Z})$ extraction from inclusive $\rm t\bar{t}$ cross sections. In summary, each source of uncertainty $\delta\sigma$ propagates into a corresponding $\alpha_{\rm S}(m_{\rm Z})$ uncertainty through $\delta\sigma/k$, where k is the slope of the fit of the theoretical cross section versus $\alpha_{\rm S}(m_{\rm Z})$. The validity of such a simple propagation of uncertainties can be demonstrated calculating first a theoretical uncertainty distribution by adding up quadratically the PDF, scale, and numerical uncertainties assuming Gaussian distributions (for the asymmetric PDF uncertainties, only the largest of the positive and negative uncertainties are used). Then, a Jpdf can be derived from the product of the theoretical and experimental distributions $f_{\rm th}(\sigma|\alpha_{\rm S}(m_{\rm Z}))$ and $f_{\rm exp}(\sigma)$. Integration over σ gives the marginalised posterior

$$P(\alpha_{\rm S}) = \int f_{\rm exp}(\sigma)\, f_{\rm th}(\sigma|\alpha_{\rm S})\, {\rm d}\sigma.$$

The expected value of the theoretical probability distribution changes linearly according to the fitted first-order polynomial, but all the theoretical and experimental uncertainties remain the same for all $\alpha_{\rm S}(m_{\rm Z})$ values. Since all the uncertainties have Gaussian distributions and the marginalisation is, in essence, a convolution, the resulting $\alpha_{\rm S}(m_{\rm Z})$ posterior will be also Gaussian, with the impact of each cross section uncertainty adding quadratically to the $\alpha_{\rm S}(m_{\rm Z})$ uncertainty. More specifically, each cross section uncertainty source $\delta\sigma$ will result in a propagated $\alpha_{\rm S}(m_{\rm Z})$ uncertainty in $\delta\sigma/k$ size, where k is the slope of the linear fit to theoretical calculations. In this demonstration, we symmetrised the PDF uncertainties for simplicity, but the $\delta\sigma/k$ prescription will be also used hereafter for the case of asymmetric uncertainties. All the extracted $\alpha_{\rm S}(m_{\rm Z})$ values, along with the uncertainty breakdowns from every source, for each system and PDF set are given in table 6. The results from the MMHT14 PDF feature the extracted $\alpha_{\rm S}(m_{\rm Z})$ values with the lowest overall uncertainty, in some cases as low as 3%.

5.3 Combination of all individual $\alpha_{\rm S}(m_{\rm Z})$ values

From the twelve $\alpha_{\rm S}(m_{\rm Z})$ extractions per PDF set listed in table 6, we can determine a single $\alpha_{\rm S}(m_{\rm Z})$ value by appropriately combining them taking into account their uncorrelated, partially-, and fully-correlated experimental and theoretical uncertainties. For this,

JHEP06(2020)018

the program CONVINO v1.2 [32] is employed, which uses a χ^2 minimisation to determine the best estimate. In the current analysis, the Neyman χ^2 code option is always used. As an independent cross-check, we confirm that, for symmetric uncertainties, the results are identical to those obtained with the BLUE method [33]. The following correlation coefficients are used:

- The integrated luminosity uncertainty is fully correlated for all $\alpha_S(m_Z)$ results obtained at the same $\sqrt{s}$, but fully uncorrelated between the two different c.m. energies.
- The experimental systematic uncertainty is partially correlated. Since the exact correlation values impact the final result, a dedicated study of the correlations is carried out in section 5.3.1.
- The experimental statistical uncertainty is fully uncorrelated among $\alpha_S(m_Z)$ extractions.
- The PDF uncertainty is partially correlated for the $\alpha_S(m_Z)$ values extracted with the same PDF set, as discussed in detail in section 5.3.2.
- The scale uncertainty is partially correlated, as explained in section 5.3.2.
- The theoretical numerical uncertainty is fully uncorrelated among $\alpha_S(m_Z)$ extractions.

By properly implementing all the uncertainties and their correlations in CONVINO, we can derive a single final combined $\alpha_S(m_Z)$ value and associated uncertainties for each PDF set.

5.3.1 Correlations among the experimental systematic uncertainties

For all the experimental measurements of the cross sections, the size of their systematic uncertainties of each type are listed in table 7. The absolute uncertainties are given in the same proportions as in table 7, but rescaled such that they add up quadratically to the total experimental systematic uncertainty listed in tables 3 and 4.

The detailed correlations between the different uncertainty sources of table 7 are listed in tables 10 to 14 of the appendix. By using the experimental systematic uncertainty breakdown and the correlations between the uncertainties, the total correlations between the experimental uncertainty sources can be calculated using the formula

$$\rho_{ij} = \frac{\sum_k \rho_{k,ij}\, \delta\sigma_{k,i}\, \delta\sigma_{k,j}}{\sqrt{\sum_k \delta\sigma_{k,i}^2}\, \sqrt{\sum_k \delta\sigma_{k,j}^2}}, \tag{5.2}$$

where the subscript k labels the uncertainty (e.g. background subtraction), and i, j denote the associated measurement (e.g. W_e^+ at 7 TeV). The calculated total correlations among experimental systematic uncertainties are given in table 15 of the appendix. Many of the propagated experimental uncertainties appear strongly correlated. To give an idea of the correlations among $\alpha_S(m_Z)$ estimates taking into account all the uncertainty sources, both experimental and theoretical, an example correlation matrix for the NNPDF3.0 set is given in table 16 of the appendix. One can see that many of the $\alpha_S(m_Z)$ values derived within a given PDF set are strongly correlated, especially across the same $\sqrt{s}$.

JHEP06(2020)018

Measurement	W_e^+	W_e^-	Z_e	W_μ^+	W_μ^-	Z_μ
7 TeV						
Lepton reconstruction and identification	1.5	1.5	1.8	0.9	0.9	—
Muon trigger inefficiency	—	—	—	0.5	0.5	0.5
Energy scale and resolution	0.5	0.6	0.12	0.19	0.25	0.35
Missing p_T scale and resolution	0.3	0.3	—	0.2	0.2	—
Background subtraction and modelling	0.3	0.5	0.14	0.4	0.5	0.28
8 TeV						
Lepton reconstruction and identification	2.8	2.5	2.8	1.0	0.9	1.1
Energy scale and resolution	0.4	0.7	0.0	0.3	0.3	0.0
Missing p_T scale and resolution	0.8	0.7	—	0.5	0.5	—
Background subtraction and modelling	0.2	0.3	0.4	0.2	0.1	0.4

Table 7. Breakdown of the experimental systematic uncertainties (in percent) for each of the $W^\pm$ and Z boson production cross section measurements at 7 and 8 TeV [13, 14].

5.3.2 Correlations among PDF and scale uncertainties

In the theoretical cross section calculations, the PDF uncertainties are in the range of a few percent, scale uncertainty up to one percent, and numerical uncertainty around half a percent (figures 3 and 4). The MCFM numerical uncertainty cannot be neglected because differences with respect to the prediction computed with the central eigenvalue/replica members are used to calculate the PDF uncertainties. The cross sections for the central PDF members have intrinsic numerical fluctuations that impact the PDF uncertainty magnitude, asymmetry, and also the correlations among theoretical uncertainties. To take this into account, a Pearson correlation coefficient is calculated for each pair of measurements and for each PDF set using the cross sections from all the PDF members that were used in calculating the PDF uncertainty. Similarly for the scale uncertainties, for each pair of measurements the Pearson correlation coefficient is calculated using the results obtained from varying the theoretical scales. The correlations are mostly in the 0.8–0.9, 0.4–0.7, 0.2–0.6, and 0.9–1.0 ranges for CT14, HERAPDF2.0, MMHT14, and NNPDF3.0, respectively. The scale correlations are around 0.6–0.9. When combining the $\alpha_S(m_Z)$ estimates, the specific correlation coefficient calculated for every specific pair of estimates is used.

6 Results and discussion

Figure 3 shows the individual results (error bars) and the final combined $\alpha_S(m_Z)$ value (coloured areas) obtained per PDF, as explained in the previous section. The width of the coloured areas in the plot indicates the size of the total propagated uncertainty in the final $\alpha_S(m_Z)$ derived for each PDF set. Table 8 lists the final $\alpha_S(m_Z)$ values determined for each PDF set through the combination of the twelve individual extractions. The total

JHEP06(2020)018

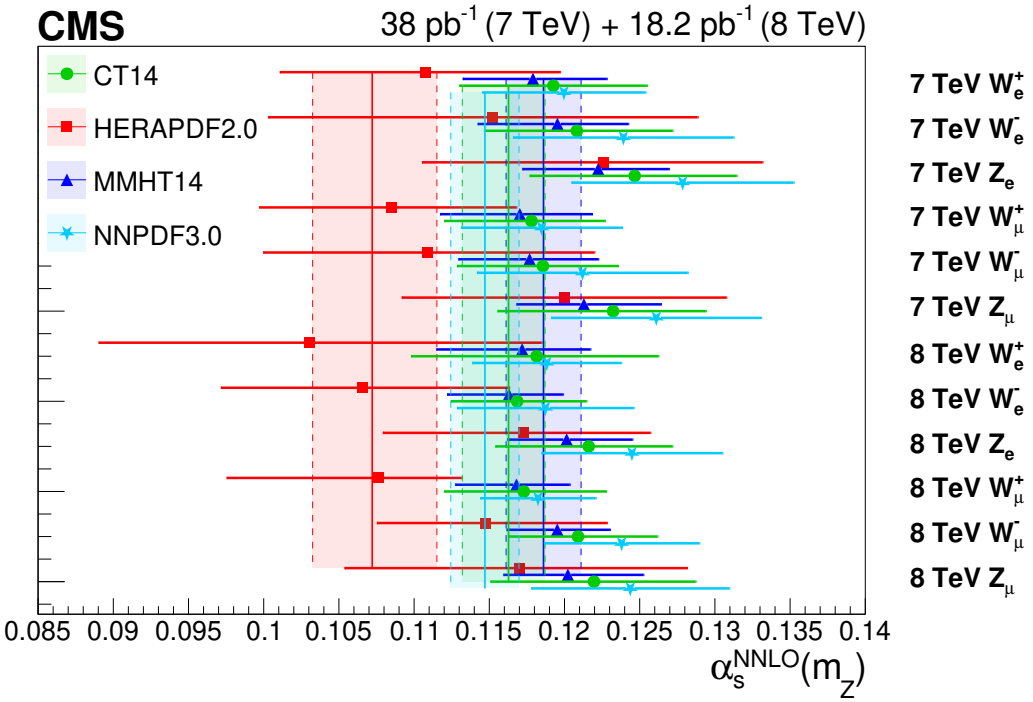

Figure 3. Individual $\alpha_S(m_Z)$ values extracted from each measured $W^{\pm}$ and Z boson production cross section (bars), and final $\alpha_S(m_Z)$ values obtained combining the twelve individual determinations (vertical coloured areas), for each PDF set.

PDF	$\alpha_S(m_Z)$	δ (stat)	δ (lumi)	δ (syst)	δ(PDF)	δ(scale)	δ(num)	χ^2/ndf
CT14	$0.1163^{+0.0024}_{-0.0031}$	0.0007	0.0013	0.0010	$^{+0.0016}_{-0.0022}$	0.0009	0.0006	13.3/11
HERAPDF2.0	$0.1072^{+0.0043}_{-0.0040}$	0.0012	0.0027	0.0012	$^{+0.0027}_{-0.0020}$	0.0012	0.0009	14.2/11
MMHT14	0.1186 ± 0.0025	0.0003	0.0018	0.0009	0.0013	0.0007	0.0002	10.2/11
NNPDF3.0	0.1147 ± 0.0023	0.0009	0.0008	0.0007	0.0014	0.0006	0.0010	29.2/11

Table 8. Strong coupling constant $\alpha_S(m_Z)$ values extracted per PDF set by combining all the individual results obtained for each $W^{\pm}$ and Z boson production cross section measurements (table 6), listed along with their total and individual uncertainties. The last column tabulates the goodness-of-fit per degree of freedom χ^2/ndf of the final single combined result compared to the twelve individual $\alpha_S(m_Z)$ extractions.

uncertainties amount to 2.0% for MMHT14 and NNPDF3.0, 2.3% for CT14, and ≈4% for HERAPDF2.0. The total $\alpha_S(m_Z)$ uncertainties derived for NNPDF3.0 are symmetric by construction, and are also symmetric at the end for MMHT14 within the accuracy given. Small asymmetries remain for the final CT14 and HERAPDF2.0 results. The dominant source of experimental uncertainty is the integrated luminosity, whereas on the theoretical side it is the knowledge of the parton densities. The last column of table 8 lists the goodness-of-fit per degree of freedom (χ^2/ndf) of the final single combined result compared to the twelve individual $\alpha_S(m_Z)$ extractions.

The $\alpha_S(m_Z)$ results obtained with HERAPDF2.0 and NNPDF3.0 show various differences with respect to those derived with the CT14 and MMHT14 sets. First, the QCD

JHEP06(2020)018

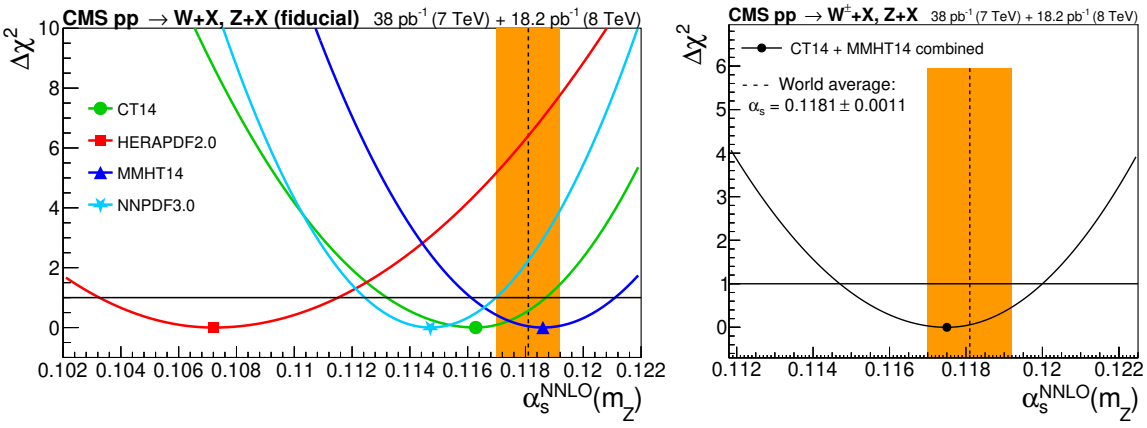

Figure 4. Final $\alpha_S(m_Z)$ values extracted for the CT14, HERAPDF2.0, MMHT14, and NNPDF3.0 PDF sets (left), and combined $\alpha_S(m_Z)$ extraction from the CT14 and MMHT14 PDFs (right), compared to the current world average (vertical orange band). The asymmetric parabolas are constructed to have a minimum at the combined value and are fitted to go through $\Delta\chi^2 = 1$ (horizontal black lines) at the one std. deviation uncertainties quoted in table 8.

PDF	$\alpha_S(m_Z)$ [7 TeV data]	$\alpha_S(m_Z)$ [8 TeV data]
CT14	$0.1158^{+0.0048}_{-0.0052}$	$0.1174^{+0.0041}_{-0.0037}$
HERAPDF2.0	0.1075 ± 0.0060	$0.1038^{+0.0107}_{-0.0073}$
MMHT14	$0.1192^{+0.0071}_{-0.0059}$	0.1184 ± 0.0029
NNPDF3.0	0.1123 ± 0.0032	0.1148 ± 0.0031
PDF	$\alpha_S(m_Z)$ [symm. PDF uncert.]	$\alpha_S(m_Z)$ [+1% uncorr. uncert.]
CT14	0.1148 ± 0.0034	$0.1169^{+0.0027}_{-0.0034}$
HERAPDF2.0	0.1119 ± 0.0056	0.1089 ± 0.0045
MMHT14	0.1185 ± 0.0028	0.1186 ± 0.0026
NNPDF3.0	0.1147 ± 0.0023	0.1155 ± 0.0029

Table 9. Sensitivity of the final $\alpha_S(m_Z)$ extractions per PDF set to various data, uncertainties, and correlation assumptions. Top rows: extractions of $\alpha_S(m_Z)$ using only the 7 and 8 TeV measurements separately. Bottom rows: extractions of $\alpha_S(m_Z)$ when symmetrising the asymmetric PDF uncertainties by taking the maximum of the negative and positive values (left), and when adding a 1% uncorrelated uncertainty to all cross sections (right).

coupling constant derived with HERAPDF2.0, $\alpha_S(m_Z) = 0.1072^{+0.0043}_{-0.0040}$, is between 1.7 and 2.7 standard deviations smaller than the rest of extractions (figure 4 left). Although as discussed later, in the context of the cross-checks described in table 9, such a disagreement is reduced when symmetrising the HERAPDF2.0 uncertainties to their maximum values. As discussed before, since the HERAPDF2.0 cross sections for $\alpha_S(m_Z) = 0.118$ tend to *overpredict* the measured $W^{\pm}$ and Z boson production cross sections (figures 1–2), a data-theory agreement can only be obtained for a value of α_S that is *reduced* compared to its

JHEP06(2020)018

default value. For all global PDF fits extracted with different α_S values as input, there exists a generic anticorrelation between the values of $\alpha_S(Q^2)$ and the parton densities evaluated at (x, Q^2), particularly, for the gluon and in turn (through perturbative evolution) for the sea quarks. It is thereby important to analyze in more detail the differences between the PDF sets for each flavour. For this purpose, a comparison study of parton densities and parton luminosities has been carried out with APFEL v2.7.1 [34]. This study indicates that the HERAPDF2.0 u-quark densities (and the overall quark-antiquark luminosities) are enhanced by about 5% compared to the rest of PDFs in the (x, Q^2) region of relevance for EW boson production. This fact increases the weight of the LO contributions to the theoretical $W^{\pm}$ and Z boson production cross sections, and thereby pushes down the cross section contributions from higher-order pQCD diagrams that are sensitive to $\alpha_S(m_Z)$. The effective result is a comparatively reduced $\alpha_S(m_Z)$ value. The level of agreement between the twelve individual and the total $\alpha_S(m_Z)$ extractions turns out to be good for this PDF set ($\chi^2/\text{ndf} \approx 1$ in table 8), because of the relatively wide span of α_S values derived and their associated large uncertainties (figure 3). Since HERAPDF2.0 uses DIS data alone, and therefore lacks the extra constraints on the PDFs provided by the LHC data, we conclude that one would need an updated refit of these parton densities to an extended set of experimental data, including LHC results, before relying on the QCD coupling constant derived following the procedure described here.

The features of the $\alpha_S(m_Z)$ results obtained with NNPDF3.0 show the opposite behaviour to those observed for the HERAPDF2.0 set. The $W^{\pm}$ and Z boson production cross sections computed with this PDF tend to *underpredict* the experimental measurements (figures 1–2), and yield an overall bad data-theory agreement ($\chi^2/\text{ndf} \approx 3$ in table 5), for the baseline $\alpha_S(m_Z) = 0.118$ coupling constant. A reproduction of the individual measurements by theory can thus be achieved only for an $\alpha_S(m_Z)$ value that is *enlarged* compared to the default value for this PDF set. Thus, many of the individual $\alpha_S(m_Z)$ extractions obtained with NNPDF3.0 have values relatively larger than those obtained for other PDFs. However, the final combined NNPDF3.0 value appears shifted down to $\alpha_S(m_Z) = 0.1147 \pm 0.0023$ (table 8), falling outside of the region around $\alpha_S(m_Z) \approx 0.120$ defined by most of the individual estimates (table 6), and, consequently, the final level of agreement of the combined and single extractions is poor ($\chi^2/\text{ndf} \approx 3$ in table 8). Such a seemingly counterintuitive behaviour is due to the presence of strong correlations among individual extractions for a fixed value of $\alpha_S(m_Z)$, and the fact that the lowest $\alpha_S(m_Z)$ values derived have smaller uncertainties than the rest, thereby pulling down the final average. The effect of a combined result lying outside of the range of the input values caused by, e.g. large underlying nonlinearities among individual estimates, is called "Peelle's pertinent puzzle" [35]. The absence of parametrisation bias in this neural-network PDF results in parton densities that can be less well constrained (have larger uncertainties) than the rest of PDFs in some regions of phase space. The same APFEL v2.7.1 study mentioned above indicates that the NNPDF3.0 quark-antiquark luminosities tend to be somewhat less precise than those from the other PDF sets in the relevant (x, Q^2) range for $W^{\pm}$ and Z production. A larger span of replicas results in nontrivial correlations among PDF uncertainties that push the final $\alpha_S(m_Z)$ value off the individual extractions for each single

JHEP06(2020)018

measurement. In any case, the latest version released (v3.1) of the NNPDF global fit [36] shows much better agreement of the theoretical EW boson cross sections with the LHC data for the central $\alpha_S(m_Z) = 0.118$ value. However, this latter NNPDF3.1 set cannot be directly employed to independently extract $\alpha_S(m_Z)$ from the CMS measurements through the approach discussed here, as this updated global fit does include already the *absolute* normalisation of a fraction of the $W^{\pm}$ and Z cross sections used in this work.

The final $\alpha_S(m_Z)$ extractions are plotted in figure 4 (left) — with (asymmetric, where needed) parabolas constructed so as to have a minimum at each final central $\alpha_S(m_Z)$ result and (one standard deviation) uncertainties matching those listed in table 8 — compared with the current world average of $\alpha_S(m_Z) = 0.1181 \pm 0.0011$ (orange band).

To analyse the robustness and stability of the final $\alpha_S(m_Z)$ extractions to the underlying data sets, their uncertainties, and correlations, we repeat the CONVINO combination varying several ingredients, as explained next. First, $\alpha_S(m_Z)$ values are extracted using separately the measurements at $\sqrt{s} = 7$ and 8 TeV alone, as shown in the top rows of table 9. This separation of data sets yields final $\alpha_S(m_Z)$ values mostly consistent with those derived from the combined ones listed in table 8, with the largest deviations from the original results being those from the 7 TeV NNPDF3.0 and 8 TeV HERAPDF2.0 extractions, with 1.0 and 0.85 standard deviations, respectively. Although the CMS luminosity studies confirm that these uncertainties are fully uncorrelated between 7 and 8 TeV, we have checked the impact of relaxing such an assumption by assuming a 0.5 correlation factor between them. Such a correlation factor results in a change of the final $\alpha_S(m_Z)$ by at most one-third of the current total uncertainty. Another cross-check is carried out by symmetrising the PDF uncertainties to their maximum value of the two (this does not apply to NNPDF3.0, because its uncertainties are symmetric by construction). The corresponding results are given in the left bottom half of table 9. Changing from asymmetric to symmetric PDF uncertainties causes the HERAPDF2.0 combined value to increase by 1.1 standard deviation, whereas all other PDF results are consistent with the default $\alpha_S(m_Z)$ extractions. Such a large sensitivity to changes in the PDF uncertainty confirms the relative lack of robustness of the $\alpha_S(m_Z)$ values derived for HERAPDF2.0 in our analysis, because the asymmetries of the PDF uncertainties can be significantly affected by random numerical errors. To further test the sensitivity of the $\alpha_S(m_Z)$ extraction to the assumptions made on the underlying $W^{\pm}$ and Z cross section uncertainties and their correlations, the original analysis is repeated by adding an uncorrelated 1% numerical uncertainty to all theoretical cross sections. Such a value accounts for possible overlooked small uncorrelated uncertainties, e.g. coming from the use of different codes for the theoretical pQCD and/or EW calculations [27]. The impact of such a change is not significant in the final results, as observed by comparing the numbers in table 8 and those in the bottom-right columns of table 9. Further similar tests and cross-checks have been carried out in a recent $\alpha_S(m_Z)$ extraction that exploits all the LHC electroweak boson data [40] with the same approach used here, which confirm these conclusions. All these systematic tests indicate that HERAPDF2.0 and NNPDF3.0 have larger variations when changing the ingredients of the combination, but for CT14 and MMHT14 the final $\alpha_S(m_Z)$ values extracted are reasonably robust within the quoted uncertainties.

JHEP06(2020)018

Among PDFs, the results obtained using MMHT14 and CT14 feature the largest sensitivity to α_S variations, i.e. they show a larger k slope, eq. (5.1), compared to those obtained with HERAPDF2.0 and NNPDF3.0 (figures 1–2). Since the uncertainty in the $\alpha_S(m_Z)$ value derived from HERAPDF2.0 is the largest (up to twice as large as some of the other extractions), because of the absence of constraining LHC input data in this HERA-only PDF fit, and since the final NNPDF3.0 result has a larger tension between the combined and individual extractions from each single measurement (table 8), we consider the values extracted with CT14, $\alpha_S(m_Z) = 0.1163^{+0.0024}_{-0.0031}$, and MMHT14, $\alpha_S(m_Z) = 0.1186 \pm 0.0025$, as the most reliable in this analysis. Providing a single final $\alpha_S(m_Z)$ value from this study is not obvious because, in general, there is no unique way to derive a final best estimate of α_S based on the results obtained from different PDF sets. An unbiased approach for combining results from different PDFs, in line with the PDG practice [1] as well as with the procedure employed to produce the PDF4LHC combined PDF set [37], is to average them without applying any further weighting. The same approach was followed also in the similar combination of QCD coupling constant values obtained from the inclusive $t\bar{t}$ cross sections [9]. By taking the straight average of the mean values and of the uncertainties of the individual CT14 and MMHT14 combinations, we obtain a final value of the QCD coupling constant at the Z pole mass, $\alpha_S(m_Z) = 0.1175^{+0.0025}_{-0.0028}$, with a total (symmetrised) uncertainty of 2.3%. Such a result compares very well with the $\alpha_S(m_Z) = 0.1177^{+0.0034}_{-0.0036}$ value, with an uncertainty of ≈3%, extracted from the theoretical analysis of top pair cross section data [9]. The right plot of figure 4 shows the $\alpha_S(m_Z)$ parabola extracted combining the CT14 and MMHT14 results. This final extraction is fully consistent with the PDG world average (orange band), and has an overall uncertainty similar to that of other recent determinations at this level of (NNLO) theoretical accuracy, such as those from EW precision fits [38], and $t\bar{t}$ cross sections [8–10].

7 Summary

We have used twelve measurements of the inclusive fiducial $W^{\pm}$ and Z production cross sections in proton-proton collisions (pp) at $\sqrt{s} = 7$ and 8 TeV, carried out in the electron and muon decay channels by the CMS experiment, to extract the value of the strong coupling constant at the Z pole mass, $\alpha_S(m_Z)$. The procedure is based on a detailed comparison of the measured electroweak boson cross sections to theoretical calculations computed at next-to-next-to-leading-order accuracy with the CT14, HERAPDF2.0, MMHT14, and NNPDF3.0 parton distribution function (PDF) sets. The overall data-theory agreement is good within the experimental and theoretical uncertainties. A χ^2-minimisation procedure has been employed to combine all twelve individual α_S extractions per PDF set, properly taking into account all individual sources of experimental and theoretical uncertainties, and their correlations. The following combined values are extracted for the four different PDFs: $\alpha_S(m_Z) = 0.1163^{+0.0024}_{-0.0031}$ (CT14), $0.1072^{+0.0043}_{-0.0040}$ (HERAPDF2.0), 0.1186 ± 0.0025 (MMHT14), and 0.1147 ± 0.0023 (NNPDF3.0). The largest propagated uncertainties are associated with the experimental integrated luminosity and theoretical intra-PDF uncertainties. Among the four extractions, the cross section calculated with the CT14 and

JHEP06(2020)018

MMHT14 sets appear as the most sensitive to the underlying α_S value and, at the same time, the derived $\alpha_S(m_Z)$ values are the most robust and stable with respect to variations in the data and theoretical cross sections, their uncertainties, and correlations. The result derived combining the CT14 and MMHT14 extractions, $\alpha_S(m_Z) = 0.1175^{+0.0025}_{-0.0028}$, has a 2.3% uncertainty that is comparable to that previously obtained in a similar analysis of the inclusive $t\bar{t}$ cross sections in pp collisions at the LHC. This extracted value is fully compatible with the current $\alpha_S(m_Z)$ world average.

Acknowledgments

We congratulate our colleagues in the CERN accelerator departments for the excellent performance of the LHC and thank the technical and administrative staffs at CERN and at other CMS institutes for their contributions to the success of the CMS effort. In addition, we gratefully acknowledge the computing centres and personnel of the Worldwide LHC Computing Grid for delivering so effectively the computing infrastructure essential to our analyses. Finally, we acknowledge the enduring support for the construction and operation of the LHC and the CMS detector provided by the following funding agencies: BMBWF and FWF (Austria); FNRS and FWO (Belgium); CNPq, CAPES, FAPERJ, FAPERGS, and FAPESP (Brazil); MES (Bulgaria); CERN; CAS, MoST, and NSFC (China); COLCIENCIAS (Colombia); MSES and CSF (Croatia); RPF (Cyprus); SENESCYT (Ecuador); MoER, ERC IUT, PUT and ERDF (Estonia); Academy of Finland, MEC, and HIP (Finland); CEA and CNRS/IN2P3 (France); BMBF, DFG, and HGF (Germany); GSRT (Greece); NKFIA (Hungary); DAE and DST (India); IPM (Iran); SFI (Ireland); INFN (Italy); MSIP and NRF (Republic of Korea); MES (Latvia); LAS (Lithuania); MOE and UM (Malaysia); BUAP, CINVESTAV, CONACYT, LNS, SEP, and UASLP-FAI (Mexico); MOS (Montenegro); MBIE (New Zealand); PAEC (Pakistan); MSHE and NSC (Poland); FCT (Portugal); JINR (Dubna); MON, RosAtom, RAS, RFBR, and NRC KI (Russia); MESTD (Serbia); SEIDI, CPAN, PCTI, and FEDER (Spain); MOSTR (Sri Lanka); Swiss Funding Agencies (Switzerland); MST (Taipei); ThEPCenter, IPST, STAR, and NSTDA (Thailand); TUBITAK and TAEK (Turkey); NASU (Ukraine); STFC (United Kingdom); DOE and NSF (U.S.A.).

Individuals have received support from the Marie-Curie programme and the European Research Council and Horizon 2020 Grant, contract Nos. 675440, 752730, and 765710 (European Union); the Leventis Foundation; the A.P. Sloan Foundation; the Alexander von Humboldt Foundation; the Belgian Federal Science Policy Office; the Fonds pour la Formation à la Recherche dans l'Industrie et dans l'Agriculture (FRIA-Belgium); the Agentschap voor Innovatie door Wetenschap en Technologie (IWT-Belgium); the F.R.S.-FNRS and FWO (Belgium) under the "Excellence of Science — EOS" — be.h project n. 30820817; the Beijing Municipal Science & Technology Commission, No. Z181100004218003; the Ministry of Education, Youth and Sports (MEYS) of the Czech Republic; the Deutsche Forschungsgemeinschaft (DFG) under Germany's Excellence Strategy — EXC 2121 "Quantum Universe" — 390833306; the Lendület ("Momentum") Programme and the János Bolyai Research Scholarship of the Hungarian Academy of Sciences, the New National Excellence

JHEP06(2020)018

		7 TeV						8 TeV					
		W_e^+	W_e^-	Z_e	W_μ^+	W_μ^-	Z_μ	W_e^+	W_e^-	Z_e	W_μ^+	W_μ^-	Z_μ
	W_e^+	1	1	1	0	0	0	1	1	1	0	0	0
	W_e^-	1	1	1	0	0	0	1	1	1	0	0	0
7	Z_e	1	1	1	0	0	0	1	1	1	0	0	0
TeV	W_μ^+	0	0	0	1	1	1	0	0	0	1	1	1
	W_μ^-	0	0	0	1	1	1	0	0	0	1	1	1
	Z_μ	0	0	0	1	1	1	0	0	0	1	1	1
	W_e^+	1	1	1	0	0	0	1	1	1	0	0	0
	W_e^-	1	1	1	0	0	0	1	1	1	0	0	0
8	Z_e	1	1	1	0	0	0	1	1	1	0	0	0
TeV	W_μ^+	0	0	0	1	1	1	0	0	0	1	1	1
	W_μ^-	0	0	0	1	1	1	0	0	0	1	1	1
	Z_μ	0	0	0	1	1	1	0	0	0	1	1	1

Table 10. Experimental systematic uncertainties: lepton reconstruction and identification correlation matrix.

Program ÚNKP, the NKFIA research grants 123842, 123959, 124845, 124850, 125105, 128713, 128786, and 129058 (Hungary); the Council of Science and Industrial Research, India; the HOMING PLUS programme of the Foundation for Polish Science, cofinanced from European Union, Regional Development Fund, the Mobility Plus programme of the Ministry of Science and Higher Education, the National Science Center (Poland), contracts Harmonia 2014/14/M/ST2/00428, Opus 2014/13/B/ST2/02543, 2014/15/B/ST2/03998, and 2015/19/B/ST2/02861, Sonata-bis 2012/07/E/ST2/01406; the National Priorities Research Program by Qatar National Research Fund; the Ministry of Science and Education, grant no. 3.2989.2017 (Russia); the Programa Estatal de Fomento de la Investigación Científica y Técnica de Excelencia María de Maeztu, grant MDM-2015-0509 and the Programa Severo Ochoa del Principado de Asturias; the Thalis and Aristeia programmes cofinanced by EU-ESF and the Greek NSRF; the Rachadapisek Sompot Fund for Postdoctoral Fellowship, Chulalongkorn University and the Chulalongkorn Academic into Its 2nd Century Project Advancement Project (Thailand); the Nvidia Corporation; the Welch Foundation, contract C-1845; and the Weston Havens Foundation (U.S.A.).

A Correlation matrices of the experimental measurements

Relevant correlation matrices of the experimental systematic uncertainties in the measurements of $W^\pm$ and Z boson production cross sections, and in their associated extractions of $\alpha_S(m_Z)$, are listed in tables 10–14 and 15–16, respectively.

JHEP06(2020)018

		7 TeV						8 TeV					
		W_e^+	W_e^-	Z_e	W_μ^+	W_μ^-	Z_μ	W_e^+	W_e^-	Z_e	W_μ^+	W_μ^-	Z_μ
	W_e^+	0	0	0	0	0	0	0	0	0	0	0	0
	W_e^-	0	0	0	0	0	0	0	0	0	0	0	0
7	Z_e	0	0	0	0	0	0	0	0	0	0	0	0
TeV	W_μ^+	0	0	0	1	1	1	0	0	0	1	1	1
	W_μ^-	0	0	0	1	1	1	0	0	0	1	1	1
	Z_μ	0	0	0	1	1	1	0	0	0	1	1	1
	W_e^+	0	0	0	0	0	0	0	0	0	0	0	0
	W_e^-	0	0	0	0	0	0	0	0	0	0	0	0
8	Z_e	0	0	0	0	0	0	0	0	0	0	0	0
TeV	W_μ^+	0	0	0	1	1	1	0	0	0	1	1	1
	W_μ^-	0	0	0	1	1	1	0	0	0	1	1	1
	Z_μ	0	0	0	1	1	1	0	0	0	1	1	1

Table 11. Experimental systematic uncertainties: muon trigger inefficiency correlation matrix [39].

		7 TeV						8 TeV					
		W_e^+	W_e^-	Z_e	W_μ^+	W_μ^-	Z_μ	W_e^+	W_e^-	Z_e	W_μ^+	W_μ^-	Z_μ
	W_e^+	1	1	1	0	0	0	1	1	1	0	0	0
	W_e^-	1	1	1	0	0	0	1	1	1	0	0	0
7	Z_e	1	1	1	0	0	0	1	1	1	0	0	0
TeV	W_μ^+	0	0	0	1	1	1	0	0	0	1	1	1
	W_μ^-	0	0	0	1	1	1	0	0	0	1	1	1
	Z_μ	0	0	0	1	1	1	0	0	0	1	1	1
	W_e^+	1	1	1	0	0	0	1	1	1	0	0	0
	W_e^-	1	1	1	0	0	0	1	1	1	0	0	0
8	Z_e	1	1	1	0	0	0	1	1	1	0	0	0
TeV	W_μ^+	0	0	0	1	1	1	0	0	0	1	1	1
	W_μ^-	0	0	0	1	1	1	0	0	0	1	1	1
	Z_μ	0	0	0	1	1	1	0	0	0	1	1	1

Table 12. Experimental systematic uncertainties: energy and momentum scale and resolution correlation matrix.

JHEP06(2020)018

		7 TeV						8 TeV					
		W_e^+	W_e^-	Z_e	W_μ^+	W_μ^-	Z_μ	W_e^+	W_e^-	Z_e	W_μ^+	W_μ^-	Z_μ
	W_e^+	1	1	0	1	1	0	1	1	0	1	1	0
	W_e^-	1	1	0	1	1	0	1	1	0	1	1	0
7	Z_e	0	0	1	0	0	0	0	0	1	0	0	0
TeV	W_μ^+	1	1	0	1	1	0	1	1	0	1	1	0
	W_μ^-	1	1	0	1	1	0	1	1	0	1	1	0
	Z_μ	0	0	0	0	0	1	0	0	1	0	0	1
	W_e^+	1	1	0	1	1	0	1	1	0	1	1	0
	W_e^-	1	1	0	1	1	0	1	1	0	1	1	0
8	Z_e	0	0	1	0	0	0	0	0	1	0	0	0
TeV	W_μ^+	1	1	0	1	1	0	1	1	0	1	1	0
	W_μ^-	1	1	0	1	1	0	1	1	0	1	1	0
	Z_μ	0	0	0	0	0	1	0	0	0	0	0	1

Table 13. Experimental systematic uncertainties: missing p_T scale and resolution correlation matrix.

		7 TeV						8 TeV					
		W_e^+	W_e^-	Z_e	W_μ^+	W_μ^-	Z_μ	W_e^+	W_e^-	Z_e	W_μ^+	W_μ^-	Z_μ
	W_e^+	1	1	0	1	1	0	1	1	0	1	1	0
	W_e^-	1	1	0	1	1	0	1	1	0	1	1	0
7	Z_e	0	0	1	0	0	1	0	0	1	0	0	1
TeV	W_μ^+	1	1	0	1	1	0	1	1	0	1	1	0
	W_μ^-	1	1	0	1	1	0	1	1	0	1	1	0
	Z_μ	0	0	1	0	0	1	0	0	1	0	0	1
	W_e^+	1	1	0	1	1	0	1	1	0	1	1	0
	W_e^-	1	1	0	1	1	0	1	1	0	1	1	0
8	Z_e	0	0	1	0	0	1	0	0	1	0	0	1
TeV	W_μ^+	1	1	0	1	1	0	1	1	0	1	1	0
	W_μ^-	1	1	0	1	1	0	1	1	0	1	1	0
	Z_μ	0	0	1	0	0	1	0	0	1	0	0	1

Table 14. Experimental systematic uncertainties: background subtraction and modelling correlation matrix.

JHEP06(2020)018

		7 TeV						8 TeV					
		W_e^+	W_e^-	Z_e	W_μ^+	W_μ^-	Z_μ	W_e^+	W_e^-	Z_e	W_μ^+	W_μ^-	Z_μ
	W_e^+	1.000	0.992	0.932	0.097	0.108	0.000	0.974	0.993	0.907	0.109	0.102	0.000
	W_e^-	0.992	1.000	0.892	0.133	0.152	0.000	0.945	0.975	0.865	0.124	0.108	0.000
7	Z_e	0.932	0.892	1.000	0.000	0.000	0.032	0.954	0.936	0.996	0.000	0.000	0.026
TeV	W_μ^+	0.097	0.133	0.000	1.000	0.996	0.414	0.072	0.084	0.000	0.850	0.821	0.743
	W_μ^-	0.108	0.152	0.000	0.996	1.000	0.423	0.074	0.090	0.000	0.842	0.809	0.712
	Z_μ	0.000	0.000	0.032	0.414	0.423	1.000	0.000	0.000	0.059	0.133	0.145	0.143
	W_e^+	0.974	0.945	0.954	0.072	0.074	0.000	1.000	0.991	0.941	0.127	0.132	0.000
	W_e^-	0.993	0.975	0.936	0.084	0.090	0.000	0.991	1.000	0.915	0.129	0.130	0.000
8	Z_e	0.907	0.865	0.996	0.000	0.000	0.059	0.941	0.915	1.000	0.000	0.000	0.048
TeV	W_μ^+	0.109	0.124	0.000	0.850	0.842	0.133	0.127	0.129	0.000	1.000	0.996	0.800
	W_μ^-	0.102	0.108	0.000	0.821	0.809	0.145	0.132	0.130	0.000	0.996	1.000	0.785
	Z_μ	0.000	0.000	0.026	0.743	0.712	0.143	0.000	0.000	0.048	0.800	0.785	1.000

Table 15. Total experimental systematic uncertainties correlations among $\alpha_S(m_Z)$ values extracted from all individual measurements at 7 and 8 TeV [13, 14] of the $W^\pm$ and Z boson production cross sections.

		7 TeV						8 TeV					
		W_e^+	W_e^-	Z_e	W_μ^+	W_μ^-	Z_μ	W_e^+	W_e^-	Z_e	W_μ^+	W_μ^-	Z_μ
	W_e^+	1.000	0.976	0.933	0.857	0.856	0.818	0.426	0.444	0.360	0.243	0.243	0.161
	W_e^-	0.976	1.000	0.938	0.871	0.880	0.835	0.417	0.435	0.353	0.248	0.254	0.168
7	Z_e	0.933	0.938	1.000	0.797	0.817	0.803	0.443	0.430	0.392	0.210	0.210	0.167
TeV	W_μ^+	0.857	0.871	0.797	1.000	0.967	0.893	0.200	0.236	0.189	0.343	0.322	0.289
	W_μ^-	0.856	0.880	0.817	0.967	1.000	0.908	0.222	0.239	0.198	0.339	0.328	0.292
	Z_μ	0.818	0.835	0.803	0.893	0.908	1.000	0.177	0.201	0.195	0.242	0.246	0.199
	W_e^+	0.426	0.417	0.443	0.200	0.222	0.177	1.000	0.940	0.794	0.664	0.685	0.467
	W_e^-	0.444	0.435	0.430	0.236	0.239	0.201	0.940	1.000	0.816	0.730	0.761	0.520
8	Z_e	0.360	0.353	0.392	0.189	0.198	0.195	0.794	0.816	1.000	0.612	0.643	0.472
TeV	W_μ^+	0.243	0.248	0.210	0.343	0.339	0.242	0.664	0.730	0.612	1.000	0.934	0.740
	W_μ^-	0.243	0.254	0.210	0.322	0.328	0.246	0.685	0.761	0.643	0.934	1.000	0.729
	Z_μ	0.161	0.168	0.167	0.289	0.292	0.199	0.467	0.520	0.472	0.740	0.729	1.000

Table 16. Total experimental and theoretical correlations between all the $\alpha_S(m_Z)$ values extracted from all measurements at 7 and 8 TeV [13, 14] of $W^\pm$ and Z boson production cross sections, obtained using the NNPDF3.0 PDF set.

JHEP06(2020)018

References

[1] Particle Data Group, *Review of Particle Physics*, *Chin. Phys.* **C 40** (2016) 100001 [INSPIRE].

[2] LHC Higgs Cross Section Working Group, *Handbook of LHC Higgs cross sections: 2. differential distributions*, CERN-2012-002 (2012) [INSPIRE].

[3] A.H. Hoang et al., *The MSR mass and the $\mathcal{O}(\Lambda_{\rm QCD})$ renormalon sum rule*, *JHEP* **04** (2018) 003 [arXiv:1704.01580] [INSPIRE].

[4] TLEP Design Study Working Group, *First Look at the Physics Case of TLEP*, *JHEP* **01** (2014) 164 [arXiv:1308.6176] [INSPIRE].

[5] D. Buttazzo et al., *Investigating the near-criticality of the Higgs boson*, *JHEP* **12** (2013) 089 [arXiv:1307.3536] [INSPIRE].

[6] D. Bourilkov, *Strong coupling running, gauge coupling unification and the scale of new physics*, *JHEP* **11** (2015) 117 [arXiv:1508.04176] [INSPIRE].

[7] F. Sannino, *α_s at LHC: Challenging asymptotic freedom*, in proceedings of the *High-Precision α_s Measurements from LHC to FCC-ee*, Geneva, Switzerland, 2–13 October 2015, pp. 11–19, [arXiv:1511.09022] [INSPIRE].

[8] CMS collaboration, *Determination of the top-quark pole mass and strong coupling constant from the $t\bar{t}$ production cross section in pp collisions at $\sqrt{s} = 7$ TeV*, *Phys. Lett.* **B 728** (2014) 496 [*Corrigendum ibid.* **B 738** (2014) 526] [arXiv:1307.1907] [INSPIRE].

[9] T. Klijnsma, S. Bethke, G. Dissertori and G.P. Salam, *Determination of the strong coupling constant $\alpha_s(m_Z)$ from measurements of the total cross section for top-antitop quark production*, *Eur. Phys. J.* **C 77** (2017) 778 [arXiv:1708.07495] [INSPIRE].

[10] CMS collaboration, *Measurement of the $t\bar{t}$ production cross section, the top quark mass and the strong coupling constant using dilepton events in pp collisions at $\sqrt{s} = 13$ TeV*, *Eur. Phys. J.* **C 79** (2019) 368 [arXiv:1812.10505] [INSPIRE].

[11] S. Alekhin et al., *Proceedings of the High-Precision α_s Measurements from LHC to FCC-ee*, Geneva, Switzerland, 2–13 October 2015, D. d'Enterria and P.Z. Skands eds., CERN, Geneva Switzerland (2015), CERN-PH-TH-2015-299 [arXiv:1512.05194] [INSPIRE].

[12] D. d'Enterria, S. Kluth eds. et al., proceedings of *α_s(2019): Precision measurements of the QCD coupling*, 11–15 February 2019, Trento, Italy, PoS ALPHAS (2019) [arXiv:1907.01435] [INSPIRE].

[13] CMS collaboration, *Measurement of the inclusive W and Z production cross sections in pp collisions at $\sqrt{s} = 7$ TeV*, *JHEP* **10** (2011) 132 [arXiv:1107.4789] [INSPIRE].

[14] CMS collaboration, *Measurement of inclusive W and Z boson production cross sections in pp collisions at $\sqrt{s} = 8$ TeV*, *Phys. Rev. Lett.* **112** (2014) 191802 [arXiv:1402.0923] [INSPIRE].

[15] R. Hamberg, W.L. van Neerven and T. Matsuura, *A complete calculation of the order α_s^2 correction to the Drell-Yan K factor*, *Nucl. Phys.* **B 359** (1991) 343 [*Erratum ibid.* **B 644** (2002) 403] [INSPIRE].

JHEP06(2020)018

[16] R. Boughezal et al., *Color singlet production at NNLO in MCFM*, *Eur. Phys. J.* **C 77** (2017) 7 [arXiv:1605.08011] [INSPIRE].

[17] S.G. Bondarenko and A.A. Sapronov, *NLO EW and QCD proton-proton cross section calculations with mcsanc-v1.01*, *Comput. Phys. Commun.* **184** (2013) 2343 [arXiv:1301.3687] [INSPIRE].

[18] C. Anastasiou, L.J. Dixon, K. Melnikov and F. Petriello, *High precision QCD at hadron colliders: Electroweak gauge boson rapidity distributions at NNLO*, *Phys. Rev.* **D 69** (2004) 094008 [hep-ph/0312266] [INSPIRE].

[19] A. Poldaru, D. d'Enterria and X. Weichen, α_S *from inclusive* $W^{\pm}$ *and* Z *cross sections in proton-proton collisions at the LHC*, in proceedings of $\alpha_S(2019)$*: Workshop on precision measurements of the QCD coupling*, Villazano, Trento, Italy, 11–15 February 2019, PoS(ALPHAS2019)013 (2019) [INSPIRE].

[20] CMS collaboration, *The CMS Experiment at the CERN LHC*, 2008 *JINST* **3** S08004 [INSPIRE].

[21] J.C. Collins, D.E. Soper and G.F. Sterman, *Factorization of Hard Processes in QCD*, *Adv. Ser. Direct. High Energy Phys.* **5** (1989) 1 [hep-ph/0409313] [INSPIRE].

[22] A. Buckley et al., *LHAPDF6: parton density access in the LHC precision era*, *Eur. Phys. J.* **C 75** (2015) 132 [arXiv:1412.7420] [INSPIRE].

[23] S. Dulat et al., *New parton distribution functions from a global analysis of quantum chromodynamics*, *Phys. Rev.* **D 93** (2016) 033006 [arXiv:1506.07443] [INSPIRE].

[24] H1 and ZEUS collaborations, *HERA Inclusive Neutral and Charged Current Cross Sections and a New PDF Fit, HERAPDF 2.0*, *Acta Phys. Polon. Supp.* **8** (2015) 957 [arXiv:1511.05402] [INSPIRE].

[25] L.A. Harland-Lang, A.D. Martin, P. Motylinski and R.S. Thorne, *Parton distributions in the LHC era: MMHT 2014 PDFs*, *Eur. Phys. J.* **C 75** (2015) 204 [arXiv:1412.3989] [INSPIRE].

[26] NNPDF collaboration, *Parton distributions for the LHC Run II*, *JHEP* **04** (2015) 040 [arXiv:1410.8849] [INSPIRE].

[27] S. Alioli et al., *Precision studies of observables in* $pp \to W \to l\nu_l$ *and* $pp \to \gamma, Z \to l^+l^-$ *processes at the LHC*, *Eur. Phys. J.* **C 77** (2017) 280 [arXiv:1606.02330] [INSPIRE].

[28] NNPDF collaboration, *Illuminating the photon content of the proton within a global PDF analysis*, *SciPost Phys.* **5** (2018) 008 [arXiv:1712.07053] [INSPIRE].

[29] D. de Florian, M. Der and I. Fabre, *QCD* $\oplus$ *QED NNLO corrections to Drell-Yan production*, *Phys. Rev.* **D 98** (2018) 094008 [arXiv:1805.12214] [INSPIRE].

[30] Y. Li and F. Petriello, *Combining QCD and electroweak corrections to dilepton production in FEWZ*, *Phys. Rev.* **D 86** (2012) 094034 [arXiv:1208.5967] [INSPIRE].

[31] A.D. Martin, W.J. Stirling, R.S. Thorne and G. Watt, *Parton distributions for the LHC*, *Eur. Phys. J.* **C 63** (2009) 189 [arXiv:0901.0002] [INSPIRE].

[32] J. Kieseler, *A method and tool for combining differential or inclusive measurements obtained with simultaneously constrained uncertainties*, *Eur. Phys. J.* **C 77** (2017) 792 [arXiv:1706.01681] [INSPIRE].

[33] R. Nisius, *On the combination of correlated estimates of a physics observable*, *Eur. Phys. J.* **C 74** (2014) 3004 [arXiv:1402.4016] [INSPIRE].

JHEP06(2020)018

[34] S. Carrazza, A. Ferrara, D. Palazzo and J. Rojo, *APFEL Web*, *J. Phys.* **G 42** (2015) 057001 [arXiv:1410.5456] [INSPIRE].

[35] D. Neudecker, R. Frühwirth, T. Kawano and H. Leeb, *Adequate treatment of correlated experimental data in nuclear data evaluations avoiding Peelle's pertinent puzzle*, *Nucl. Data Sheets* **118** (2014) 364.

[36] NNPDF collaboration, *Parton distributions from high-precision collider data*, *Eur. Phys. J.* **C 77** (2017) 663 [arXiv:1706.00428] [INSPIRE].

[37] J. Butterworth et al., *PDF4LHC recommendations for LHC Run II*, *J. Phys.* **G 43** (2016) 023001 [arXiv:1510.03865] [INSPIRE].

[38] J. Haller, A. Hoecker, R. Kogler, K. Mönig, T. Peiffer and J. Stelzer, *Update of the global electroweak fit and constraints on two-Higgs-doublet models*, *Eur. Phys. J.* **C 78** (2018) 675 [arXiv:1803.01853] [INSPIRE].

[39] CMS collaboration, *The CMS trigger system*, 2017 *JINST* **12** P01020 [arXiv:1609.02366] [INSPIRE].

[40] D. d'Enterria and A. Poldaru, *Strong coupling $\alpha_s(m_Z)$ extraction from a combined NNLO analysis of inclusive electroweak boson cross sections at hadron colliders*, arXiv:1912.11733 [INSPIRE].

JHEP06(2020)018

The CMS collaboration

Yerevan Physics Institute, Yerevan, Armenia

A.M. Sirunyan[†], A. Tumasyan

Institut für Hochenergiephysik, Wien, Austria

W. Adam, F. Ambrogi, T. Bergauer, M. Dragicevic, J. Erö, A. Escalante Del Valle, M. Flechl, R. Frühwirth[1], M. Jeitler[1], N. Krammer, I. Krätschmer, D. Liko, T. Madlener, I. Mikulec, N. Rad, J. Schieck[1], R. Schöfbeck, M. Spanring, W. Waltenberger, C.-E. Wulz[1], M. Zarucki

Institute for Nuclear Problems, Minsk, Belarus

V. Drugakov, V. Mossolov, J. Suarez Gonzalez

Universiteit Antwerpen, Antwerpen, Belgium

M.R. Darwish, E.A. De Wolf, D. Di Croce, X. Janssen, A. Lelek, M. Pieters, H. Rejeb Sfar, H. Van Haevermaet, P. Van Mechelen, S. Van Putte, N. Van Remortel

Vrije Universiteit Brussel, Brussel, Belgium

F. Blekman, E.S. Bols, S.S. Chhibra, J. D'Hondt, J. De Clercq, D. Lontkovskyi, S. Lowette, I. Marchesini, S. Moortgat, Q. Python, S. Tavernier, W. Van Doninck, P. Van Mulders

Université Libre de Bruxelles, Bruxelles, Belgium

D. Beghin, B. Bilin, B. Clerbaux, G. De Lentdecker, H. Delannoy, B. Dorney, L. Favart, A. Grebenyuk, A.K. Kalsi, L. Moureaux, A. Popov, N. Postiau, E. Starling, L. Thomas, C. Vander Velde, P. Vanlaer, D. Vannerom

Ghent University, Ghent, Belgium

T. Cornelis, D. Dobur, I. Khvastunov[2], M. Niedziela, C. Roskas, K. Skovpen, M. Tytgat, W. Verbeke, B. Vermassen, M. Vit

Université Catholique de Louvain, Louvain-la-Neuve, Belgium

O. Bondu, G. Bruno, C. Caputo, P. David, C. Delaere, M. Delcourt, A. Giammanco, V. Lemaitre, J. Prisciandaro, A. Saggio, M. Vidal Marono, P. Vischia, J. Zobec

Centro Brasileiro de Pesquisas Fisicas, Rio de Janeiro, Brazil

G.A. Alves, G. Correia Silva, C. Hensel, A. Moraes

Universidade do Estado do Rio de Janeiro, Rio de Janeiro, Brazil

E. Belchior Batista Das Chagas, W. Carvalho, J. Chinellato[3], E. Coelho, E.M. Da Costa, G.G. Da Silveira[4], D. De Jesus Damiao, C. De Oliveira Martins, S. Fonseca De Souza, L.M. Huertas Guativa, H. Malbouisson, J. Martins[5], D. Matos Figueiredo, M. Medina Jaime[6], M. Melo De Almeida, C. Mora Herrera, L. Mundim, H. Nogima, W.L. Prado Da Silva, P. Rebello Teles, L.J. Sanchez Rosas, A. Santoro, A. Sznajder, M. Thiel, E.J. Tonelli Manganote[3], F. Torres Da Silva De Araujo, A. Vilela Pereira

JHEP06(2020)018

Universidade Estadual Paulista[a], Universidade Federal do ABC[b], S ao Paulo, Brazil

C.A. Bernardes[a], L. Calligaris[a], T.R. Fernandez Perez Tomei[a], E.M. Gregores[b], D.S. Lemos, P.G. Mercadante[b], S.F. Novaes[a], SandraS. Padula[a]

Institute for Nuclear Research and Nuclear Energy, Bulgarian Academy of Sciences, Sofia, Bulgaria

A. Aleksandrov, G. Antchev, R. Hadjiiska, P. Iaydjiev, M. Misheva, M. Rodozov, M. Shopova, G. Sultanov

University of Sofia, Sofia, Bulgaria

M. Bonchev, A. Dimitrov, T. Ivanov, L. Litov, B. Pavlov, P. Petkov, A. Petrov

Beihang University, Beijing, China

W. Fang[7], X. Gao[7], L. Yuan

Department of Physics, Tsinghua University, Beijing, China

M. Ahmad, Z. Hu, Y. Wang

Institute of High Energy Physics, Beijing, China

G.M. Chen[8], H.S. Chen[8], M. Chen, C.H. Jiang, D. Leggat, H. Liao, Z. Liu, A. Spiezia, J. Tao, E. Yazgan, H. Zhang, S. Zhang[8], J. Zhao

State Key Laboratory of Nuclear Physics and Technology, Peking University, Beijing, China

A. Agapitos, Y. Ban, G. Chen, A. Levin, J. Li, L. Li, Q. Li, Y. Mao, S.J. Qian, D. Wang, Q. Wang

Zhejiang University, Hangzhou, China

M. Xiao

Universidad de Los Andes, Bogota, Colombia

C. Avila, A. Cabrera, C. Florez, C.F. González Hernández, M.A. Segura Delgado

Universidad de Antioquia, Medellin, Colombia

J. Mejia Guisao, J.D. Ruiz Alvarez, C.A. Salazar González, N. Vanegas Arbelaez

University of Split, Faculty of Electrical Engineering, Mechanical Engineering and Naval Architecture, Split, Croatia

D. Giljanović, N. Godinovic, D. Lelas, I. Puljak, T. Sculac

University of Split, Faculty of Science, Split, Croatia

Z. Antunovic, M. Kovac

Institute Rudjer Boskovic, Zagreb, Croatia

V. Brigljevic, D. Ferencek, K. Kadija, B. Mesic, M. Roguljic, A. Starodumov[9], T. Susa

University of Cyprus, Nicosia, Cyprus

M.W. Ather, A. Attikis, E. Erodotou, A. Ioannou, M. Kolosova, S. Konstantinou, G. Mavromanolakis, J. Mousa, C. Nicolaou, F. Ptochos, P.A. Razis, H. Rykaczewski, H. Saka, D. Tsiakkouri

JHEP06(2020)018

Charles University, Prague, Czech Republic
M. Finger[10], M. Finger Jr.[10], A. Kveton, J. Tomsa

Escuela Politecnica Nacional, Quito, Ecuador
E. Ayala

Universidad San Francisco de Quito, Quito, Ecuador
E. Carrera Jarrin

Academy of Scientific Research and Technology of the Arab Republic of Egypt, Egyptian Network of High Energy Physics, Cairo, Egypt
Y. Assran[11,12], S. Elgammal[12]

National Institute of Chemical Physics and Biophysics, Tallinn, Estonia
S. Bhowmik, A. Carvalho Antunes De Oliveira, R.K. Dewanjee, K. Ehataht, M. Kadastik, A. Poldaru, M. Raidal, C. Veelken

Department of Physics, University of Helsinki, Helsinki, Finland
P. Eerola, L. Forthomme, H. Kirschenmann, K. Osterberg, M. Voutilainen

Helsinki Institute of Physics, Helsinki, Finland
F. Garcia, J. Havukainen, J.K. Heikkilä, V. Karimäki, M.S. Kim, R. Kinnunen, T. Lampén, K. Lassila-Perini, S. Laurila, S. Lehti, T. Lindén, H. Siikonen, E. Tuominen, J. Tuominiemi

Lappeenranta University of Technology, Lappeenranta, Finland
P. Luukka, T. Tuuva

IRFU, CEA, Université Paris-Saclay, Gif-sur-Yvette, France
M. Besancon, F. Couderc, M. Dejardin, D. Denegri, B. Fabbro, J.L. Faure, F. Ferri, S. Ganjour, A. Givernaud, P. Gras, G. Hamel de Monchenault, P. Jarry, C. Leloup, B. Lenzi, E. Locci, J. Malcles, J. Rander, A. Rosowsky, M.Ö. Sahin, A. Savoy-Navarro[13], M. Titov, G.B. Yu

Laboratoire Leprince-Ringuet, CNRS/IN2P3, Ecole Polytechnique, Institut Polytechnique de Paris
S. Ahuja, C. Amendola, F. Beaudette, P. Busson, C. Charlot, B. Diab, G. Falmagne, R. Granier de Cassagnac, I. Kucher, A. Lobanov, C. Martin Perez, M. Nguyen, C. Ochando, P. Paganini, J. Rembser, R. Salerno, J.B. Sauvan, Y. Sirois, A. Zabi, A. Zghiche

Université de Strasbourg, CNRS, IPHC UMR 7178, Strasbourg, France
J.-L. Agram[14], J. Andrea, D. Bloch, G. Bourgatte, J.-M. Brom, E.C. Chabert, C. Collard, E. Conte[14], J.-C. Fontaine[14], D. Gelé, U. Goerlach, C. Grimault, M. Jansová, A.-C. Le Bihan, N. Tonon, P. Van Hove

Centre de Calcul de l'Institut National de Physique Nucleaire et de Physique des Particules, CNRS/IN2P3, Villeurbanne, France
S. Gadrat

JHEP06(2020)018

Université de Lyon, Université Claude Bernard Lyon 1, CNRS-IN2P3, Institut de Physique Nucléaire de Lyon, Villeurbanne, France

S. Beauceron, C. Bernet, G. Boudoul, C. Camen, A. Carle, N. Chanon, R. Chierici, D. Contardo, P. Depasse, H. El Mamouni, J. Fay, S. Gascon, M. Gouzevitch, B. Ille, Sa. Jain, I.B. Laktineh, H. Lattaud, A. Lesauvage, M. Lethuillier, L. Mirabito, S. Perries, V. Sordini, L. Torterotot, G. Touquet, M. Vander Donckt, S. Viret

Georgian Technical University, Tbilisi, Georgia

G. Adamov

Tbilisi State University, Tbilisi, Georgia

Z. Tsamalaidze[10]

RWTH Aachen University, I. Physikalisches Institut, Aachen, Germany

C. Autermann, L. Feld, K. Klein, M. Lipinski, D. Meuser, A. Pauls, M. Preuten, M.P. Rauch, J. Schulz, M. Teroerde

RWTH Aachen University, III. Physikalisches Institut A, Aachen, Germany

M. Erdmann, B. Fischer, S. Ghosh, T. Hebbeker, K. Hoepfner, H. Keller, L. Mastrolorenzo, M. Merschmeyer, A. Meyer, P. Millet, G. Mocellin, S. Mondal, S. Mukherjee, D. Noll, A. Novak, T. Pook, A. Pozdnyakov, T. Quast, M. Radziej, Y. Rath, H. Reithler, J. Roemer, A. Schmidt, S.C. Schuler, A. Sharma, S. Wiedenbeck, S. Zaleski

RWTH Aachen University, III. Physikalisches Institut B, Aachen, Germany

G. Flügge, W. Haj Ahmad[15], O. Hlushchenko, T. Kress, T. Müller, A. Nowack, C. Pistone, O. Pooth, D. Roy, H. Sert, A. Stahl[16]

Deutsches Elektronen-Synchrotron, Hamburg, Germany

M. Aldaya Martin, P. Asmuss, I. Babounikau, H. Bakhshiansohi, K. Beernaert, O. Behnke, A. Bermúdez Martínez, A.A. Bin Anuar, K. Borras[17], V. Botta, A. Campbell, A. Cardini, P. Connor, S. Consuegra Rodríguez, C. Contreras-Campana, V. Danilov, A. De Wit, M.M. Defranchis, C. Diez Pardos, D. Domínguez Damiani, G. Eckerlin, D. Eckstein, T. Eichhorn, A. Elwood, E. Eren, E. Gallo[18], A. Geiser, A. Grohsjean, M. Guthoff, M. Haranko, A. Harb, A. Jafari, N.Z. Jomhari, H. Jung, A. Kasem[17], M. Kasemann, H. Kaveh, J. Keaveney, C. Kleinwort, J. Knolle, D. Krücker, W. Lange, T. Lenz, J. Lidrych, W. Lohmann[19], R. Mankel, I.-A. Melzer-Pellmann, A.B. Meyer, M. Meyer, M. Missiroli, J. Mnich, A. Mussgiller, V. Myronenko, D. Pérez Adán, S.K. Pflitsch, D. Pitzl, A. Raspereza, A. Saibel, M. Savitskyi, V. Scheurer, P. Schütze, C. Schwanenberger, R. Shevchenko, A. Singh, R.E. Sosa Ricardo, H. Tholen, O. Turkot, A. Vagnerini, M. Van De Klundert, R. Walsh, Y. Wen, K. Wichmann, C. Wissing, O. Zenaiev, R. Zlebcik

University of Hamburg, Hamburg, Germany

R. Aggleton, S. Bein, L. Benato, A. Benecke, T. Dreyer, A. Ebrahimi, F. Feindt, A. Fröhlich, C. Garbers, E. Garutti, D. Gonzalez, P. Gunnellini, J. Haller, A. Hinzmann, A. Karavdina, G. Kasieczka, R. Klanner, R. Kogler, N. Kovalchuk, S. Kurz, V. Kutzner, J. Lange, T. Lange, A. Malara, J. Multhaup, C.E.N. Niemeyer, A. Reimers,

JHEP06(2020)018

O. Rieger, P. Schleper, S. Schumann, J. Schwandt, J. Sonneveld, H. Stadie, G. Steinbrück, B. Vormwald, I. Zoi

Karlsruher Institut fuer Technologie, Karlsruhe, Germany

M. Akbiyik, M. Baselga, S. Baur, T. Berger, E. Butz, R. Caspart, T. Chwalek, W. De Boer, A. Dierlamm, K. El Morabit, N. Faltermann, M. Giffels, A. Gottmann, F. Hartmann[16], C. Heidecker, U. Husemann, S. Kudella, S. Maier, S. Mitra, M.U. Mozer, D. Müller, Th. Müller, M. Musich, A. Nürnberg, G. Quast, K. Rabbertz, D. Schäfer, M. Schröder, I. Shvetsov, H.J. Simonis, R. Ulrich, M. Wassmer, M. Weber, C. Wöhrmann, R. Wolf, S. Wozniewski

Institute of Nuclear and Particle Physics (INPP), NCSR Demokritos, Aghia Paraskevi, Greece

G. Anagnostou, P. Asenov, G. Daskalakis, T. Geralis, A. Kyriakis, D. Loukas, G. Paspalaki

National and Kapodistrian University of Athens, Athens, Greece

M. Diamantopoulou, G. Karathanasis, P. Kontaxakis, A. Manousakis-katsikakis, A. Panagiotou, I. Papavergou, N. Saoulidou, A. Stakia, K. Theofilatos, K. Vellidis, E. Vourliotis

National Technical University of Athens, Athens, Greece

G. Bakas, K. Kousouris, I. Papakrivopoulos, G. Tsipolitis, A. Zacharopoulou

University of Ioánnina, Ioánnina, Greece

I. Evangelou, C. Foudas, P. Gianneios, P. Katsoulis, P. Kokkas, S. Mallios, K. Manitara, N. Manthos, I. Papadopoulos, J. Strologas, F.A. Triantis, D. Tsitsonis

MTA-ELTE Lendület CMS Particle and Nuclear Physics Group, Eötvös Loránd University, Budapest, Hungary

M. Bartók[20], R. Chudasama, M. Csanad, P. Major, K. Mandal, A. Mehta, G. Pasztor, O. Surányi, G.I. Veres

Wigner Research Centre for Physics, Budapest, Hungary

G. Bencze, C. Hajdu, D. Horvath[21], F. Sikler, V. Veszpremi, G. Vesztergombi[†]

Institute of Nuclear Research ATOMKI, Debrecen, Hungary

N. Beni, S. Czellar, J. Karancsi[20], J. Molnar, Z. Szillasi

Institute of Physics, University of Debrecen, Debrecen, Hungary

P. Raics, D. Teyssier, Z.L. Trocsanyi, B. Ujvari

Eszterhazy Karoly University, Karoly Robert Campus, Gyongyos, Hungary

T. Csorgo, W.J. Metzger, F. Nemes, T. Novak

Indian Institute of Science (IISc), Bangalore, India

S. Choudhury, J.R. Komaragiri, P.C. Tiwari

National Institute of Science Education and Research, HBNI, Bhubaneswar, India

S. Bahinipati[23], C. Kar, G. Kole, P. Mal, V.K. Muraleedharan Nair Bindhu, A. Nayak[24], D.K. Sahoo[23], S.K. Swain

JHEP06(2020)018

Panjab University, Chandigarh, India
S. Bansal, S.B. Beri, V. Bhatnagar, S. Chauhan, N. Dhingra[25], R. Gupta, A. Kaur, M. Kaur, S. Kaur, P. Kumari, M. Lohan, M. Meena, K. Sandeep, S. Sharma, J.B. Singh, A.K. Virdi

University of Delhi, Delhi, India
A. Bhardwaj, B.C. Choudhary, R.B. Garg, M. Gola, S. Keshri, Ashok Kumar, M. Naimuddin, P. Priyanka, K. Ranjan, Aashaq Shah, R. Sharma

Saha Institute of Nuclear Physics, HBNI, Kolkata, India
R. Bhardwaj[26], M. Bharti[26], R. Bhattacharya, S. Bhattacharya, U. Bhawandeep[26], D. Bhowmik, S. Dutta, S. Ghosh, B. Gomber[27], M. Maity[28], K. Mondal, S. Nandan, A. Purohit, P.K. Rout, G. Saha, S. Sarkar, T. Sarkar[28], M. Sharan, B. Singh[26], S. Thakur[26]

Indian Institute of Technology Madras, Madras, India
P.K. Behera, S.C. Behera, P. Kalbhor, A. Muhammad, P.R. Pujahari, A. Sharma, A.K. Sikdar

Bhabha Atomic Research Centre, Mumbai, India
D. Dutta, V. Jha, D.K. Mishra, P.K. Netrakanti, L.M. Pant, P. Shukla

Tata Institute of Fundamental Research-A, Mumbai, India
T. Aziz, M.A. Bhat, S. Dugad, G.B. Mohanty, N. Sur, RavindraKumar Verma

Tata Institute of Fundamental Research-B, Mumbai, India
S. Banerjee, S. Bhattacharya, S. Chatterjee, P. Das, M. Guchait, S. Karmakar, S. Kumar, G. Majumder, K. Mazumdar, N. Sahoo, S. Sawant

Indian Institute of Science Education and Research (IISER), Pune, India
S. Dube, B. Kansal, A. Kapoor, K. Kothekar, S. Pandey, A. Rane, A. Rastogi, S. Sharma

Institute for Research in Fundamental Sciences (IPM), Tehran, Iran
S. Chenarani, S.M. Etesami, M. Khakzad, M. Mohammadi Najafabadi, M. Naseri, F. Rezaei Hosseinabadi

University College Dublin, Dublin, Ireland
M. Felcini, M. Grunewald

INFN Sezione di Bari[a], Università di Bari[b], Politecnico di Bari[c], Bari, Italy
M. Abbrescia[a,b], R. Aly[a,b,29], C. Calabria[a,b], A. Colaleo[a], D. Creanza[a,c], L. Cristella[a,b], N. De Filippis[a,c], M. De Palma[a,b], A. Di Florio[a,b], W. Elmetenawee[a,b], L. Fiore[a], A. Gelmi[a,b], G. Iaselli[a,c], M. Ince[a,b], S. Lezki[a,b], G. Maggi[a,c], M. Maggi[a], J.A. Merlin[a], G. Miniello[a,b], S. My[a,b], S. Nuzzo[a,b], A. Pompili[a,b], G. Pugliese[a,c], R. Radogna[a], A. Ranieri[a], G. Selvaggi[a,b], L. Silvestris[a], F.M. Simone[a,b], R. Venditti[a], P. Verwilligen[a]

INFN Sezione di Bologna[a], Università di Bologna[b], Bologna, Italy
G. Abbiendi[a], C. Battilana[a,b], D. Bonacorsi[a,b], L. Borgonovi[a,b], S. Braibant-Giacomelli[a,b], R. Campanini[a,b], P. Capiluppi[a,b], A. Castro[a,b], F.R. Cavallo[a], C. Ciocca[a], G. Codispoti[a,b], M. Cuffiani[a,b], G.M. Dallavalle[a], F. Fabbri[a], A. Fanfani[a,b], E. Fontanesi[a,b], P. Giacomelli[a],

JHEP06(2020)018

C. Grandi[a], L. Guiducci[a,b], F. Iemmi[a,b], S. Lo Meo[a,30], S. Marcellini[a], G. Masetti[a], F.L. Navarria[a,b], A. Perrotta[a], F. Primavera[a,b], A.M. Rossi[a,b], T. Rovelli[a,b], G.P. Siroli[a,b], N. Tosi[a]

INFN Sezione di Catania[a], Università di Catania[b], Catania, Italy

S. Albergo[a,b,31], S. Costa[a,b], A. Di Mattia[a], R. Potenza[a,b], A. Tricomi[a,b,31], C. Tuve[a,b]

INFN Sezione di Firenze[a], Università di Firenze[b], Firenze, Italy

G. Barbagli[a], A. Cassese, R. Ceccarelli, V. Ciulli[a,b], C. Civinini[a], R. D'Alessandro[a,b], F. Fiori[a,c], E. Focardi[a,b], G. Latino[a,b], P. Lenzi[a,b], M. Meschini[a], S. Paoletti[a], G. Sguazzoni[a], L. Viliani[a]

INFN Laboratori Nazionali di Frascati, Frascati, Italy

L. Benussi, S. Bianco, D. Piccolo

INFN Sezione di Genova[a], Università di Genova[b], Genova, Italy

M. Bozzo[a,b], F. Ferro[a], R. Mulargia[a,b], E. Robutti[a], S. Tosi[a,b]

INFN Sezione di Milano-Bicocca[a], Università di Milano-Bicocca[b], Milano, Italy

A. Benaglia[a], A. Beschi[a,b], F. Brivio[a,b], V. Ciriolo[a,b,16], M.E. Dinardo[a,b], P. Dini[a], S. Gennai[a], A. Ghezzi[a,b], P. Govoni[a,b], L. Guzzi[a,b], M. Malberti[a], S. Malvezzi[a], D. Menasce[a], F. Monti[a,b], L. Moroni[a], M. Paganoni[a,b], D. Pedrini[a], S. Ragazzi[a,b], T. Tabarelli de Fatis[a,b], D. Valsecchi[a,b], D. Zuolo[a,b]

INFN Sezione di Napoli[a], Università di Napoli 'Federico II'[b], Napoli, Italy, Università della Basilicata[c], Potenza, Italy, Università G. Marconi[d], Roma, Italy

S. Buontempo[a], N. Cavallo[a,c], A. De Iorio[a,b], A. Di Crescenzo[a,b], F. Fabozzi[a,c], F. Fienga[a], G. Galati[a], A.O.M. Iorio[a,b], L. Layer[a,b], L. Lista[a,b], S. Meola[a,d,16], P. Paolucci[a,16], B. Rossi[a], C. Sciacca[a,b], E. Voevodina[a,b]

INFN Sezione di Padova[a], Università di Padova[b], Padova, Italy, Università di Trento[c], Trento, Italy

P. Azzi[a], N. Bacchetta[a], D. Bisello[a,b], A. Boletti[a,b], A. Bragagnolo[a,b], R. Carlin[a,b], P. Checchia[a], P. De Castro Manzano[a], T. Dorigo[a], U. Dosselli[a], F. Gasparini[a,b], U. Gasparini[a,b], A. Gozzelino[a], S.Y. Hoh[a,b], M. Margoni[a,b], A.T. Meneguzzo[a,b], J. Pazzini[a,b], M. Presilla[b], P. Ronchese[a,b], R. Rossin[a,b], F. Simonetto[a,b], A. Tiko[a], M. Tosi[a,b], M. Zanetti[a,b], P. Zotto[a,b], A. Zucchetta[a,b], G. Zumerle[a,b]

INFN Sezione di Pavia[a], Università di Pavia[b], Pavia, Italy

A. Braghieri[a], D. Fiorina[a,b], P. Montagna[a,b], S.P. Ratti[a,b], V. Re[a], M. Ressegotti[a,b], C. Riccardi[a,b], P. Salvini[a], I. Vai[a], P. Vitulo[a,b]

INFN Sezione di Perugia[a], Università di Perugia[b], Perugia, Italy

M. Biasini[a,b], G.M. Bilei[a], D. Ciangottini[a,b], L. Fanò[a,b], P. Lariccia[a,b], R. Leonardi[a,b], E. Manoni[a], G. Mantovani[a,b], V. Mariani[a,b], M. Menichelli[a], A. Rossi[a,b], A. Santocchia[a,b], D. Spiga[a]

JHEP06(2020)018

INFN Sezione di Pisa[a], Università di Pisa[b], Scuola Normale Superiore di Pisa[c], Pisa, Italy

K. Androsov[a], P. Azzurri[a], G. Bagliesi[a], V. Bertacchi[a,c], L. Bianchini[a], T. Boccali[a], R. Castaldi[a], M.A. Ciocci[a,b], R. Dell'Orso[a], S. Donato[a], L. Giannini[a,c], A. Giassi[a], M.T. Grippo[a], F. Ligabue[a,c], E. Manca[a,c], G. Mandorli[a,c], A. Messineo[a,b], F. Palla[a], A. Rizzi[a,b], G. Rolandi[32], S. Roy Chowdhury, A. Scribano[a], P. Spagnolo[a], R. Tenchini[a], G. Tonelli[a,b], N. Turini, A. Venturi[a], P.G. Verdini[a]

INFN Sezione di Roma[a], Sapienza Università di Roma[b], Rome, Italy

F. Cavallari[a], M. Cipriani[a,b], D. Del Re[a,b], E. Di Marco[a], M. Diemoz[a], E. Longo[a,b], P. Meridiani[a], G. Organtini[a,b], F. Pandolfi[a], R. Paramatti[a,b], C. Quaranta[a,b], S. Rahatlou[a,b], C. Rovelli[a], F. Santanastasio[a,b], L. Soffi[a,b]

INFN Sezione di Torino[a], Università di Torino[b], Torino, Italy, Università del Piemonte Orientale[c], Novara, Italy

N. Amapane[a,b], R. Arcidiacono[a,c], S. Argiro[a,b], M. Arneodo[a,c], N. Bartosik[a], R. Bellan[a,b], A. Bellora, C. Biino[a], A. Cappati[a,b], N. Cartiglia[a], S. Cometti[a], M. Costa[a,b], R. Covarelli[a,b], N. Demaria[a], B. Kiani[a,b], F. Legger, C. Mariotti[a], S. Maselli[a], E. Migliore[a,b], V. Monaco[a,b], E. Monteil[a,b], M. Monteno[a], M.M. Obertino[a,b], G. Ortona[a,b], L. Pacher[a,b], N. Pastrone[a], M. Pelliccioni[a], G.L. Pinna Angioni[a,b], A. Romero[a,b], M. Ruspa[a,c], R. Salvatico[a,b], V. Sola[a], A. Solano[a,b], D. Soldi[a,b], A. Staiano[a], D. Trocino[a,b]

INFN Sezione di Trieste[a], Università di Trieste[b], Trieste, Italy

S. Belforte[a], V. Candelise[a,b], M. Casarsa[a], F. Cossutti[a], A. Da Rold[a,b], G. Della Ricca[a,b], F. Vazzoler[a,b], A. Zanetti[a]

Kyungpook National University, Daegu, Korea

B. Kim, D.H. Kim, G.N. Kim, J. Lee, S.W. Lee, C.S. Moon, Y.D. Oh, S.I. Pak, S. Sekmen, D.C. Son, Y.C. Yang

Chonnam National University, Institute for Universe and Elementary Particles, Kwangju, Korea

H. Kim, D.H. Moon, G. Oh

Hanyang University, Seoul, Korea

B. Francois, T.J. Kim, J. Park

Korea University, Seoul, Korea

S. Cho, S. Choi, Y. Go, S. Ha, B. Hong, K. Lee, K.S. Lee, J. Lim, J. Park, S.K. Park, Y. Roh, J. Yoo

Kyung Hee University, Department of Physics

J. Goh

Sejong University, Seoul, Korea

H.S. Kim

JHEP06(2020)018

Seoul National University, Seoul, Korea
J. Almond, J.H. Bhyun, J. Choi, S. Jeon, J. Kim, J.S. Kim, H. Lee, K. Lee, S. Lee, K. Nam, M. Oh, S.B. Oh, B.C. Radburn-Smith, U.K. Yang, H.D. Yoo, I. Yoon

University of Seoul, Seoul, Korea
D. Jeon, J.H. Kim, J.S.H. Lee, I.C. Park, I.J Watson

Sungkyunkwan University, Suwon, Korea
Y. Choi, C. Hwang, Y. Jeong, J. Lee, Y. Lee, I. Yu

Riga Technical University, Riga, Latvia
V. Veckalns[33]

Vilnius University, Vilnius, Lithuania
V. Dudenas, A. Juodagalvis, A. Rinkevicius, G. Tamulaitis, J. Vaitkus

National Centre for Particle Physics, Universiti Malaya, Kuala Lumpur, Malaysia
F. Mohamad Idris[34], W.A.T. Wan Abdullah, M.N. Yusli, Z. Zolkapli

Universidad de Sonora (UNISON), Hermosillo, Mexico
J.F. Benitez, A. Castaneda Hernandez, J.A. Murillo Quijada, L. Valencia Palomo

Centro de Investigacion y de Estudios Avanzados del IPN, Mexico City, Mexico
H. Castilla-Valdez, E. De La Cruz-Burelo, I. Heredia-De La Cruz[35], R. Lopez-Fernandez, A. Sanchez-Hernandez

Universidad Iberoamericana, Mexico City, Mexico
S. Carrillo Moreno, C. Oropeza Barrera, M. Ramirez-Garcia, F. Vazquez Valencia

Benemerita Universidad Autonoma de Puebla, Puebla, Mexico
J. Eysermans, I. Pedraza, H.A. Salazar Ibarguen, C. Uribe Estrada

Universidad Autónoma de San Luis Potosí, San Luis Potosí, Mexico
A. Morelos Pineda

University of Montenegro, Podgorica, Montenegro
J. Mijuskovic[2], N. Raicevic

University of Auckland, Auckland, New Zealand
D. Krofcheck

University of Canterbury, Christchurch, New Zealand
S. Bheesette, P.H. Butler, P. Lujan

National Centre for Physics, Quaid-I-Azam University, Islamabad, Pakistan
A. Ahmad, M. Ahmad, M.I.M. Awan, Q. Hassan, H.R. Hoorani, W.A. Khan, M.A. Shah, M. Shoaib, M. Waqas

AGH University of Science and Technology Faculty of Computer Science, Electronics and Telecommunications, Krakow, Poland
V. Avati, L. Grzanka, M. Malawski

JHEP06(2020)018

National Centre for Nuclear Research, Swierk, Poland
H. Bialkowska, M. Bluj, B. Boimska, M. Górski, M. Kazana, M. Szleper, P. Zalewski

Institute of Experimental Physics, Faculty of Physics, University of Warsaw, Warsaw, Poland
K. Bunkowski, A. Byszuk[36], K. Doroba, A. Kalinowski, M. Konecki, J. Krolikowski, M. Olszewski, M. Walczak

Laboratório de Instrumentaç ao e Física Experimental de Partículas, Lisboa, Portugal
M. Araujo, P. Bargassa, D. Bastos, A. Di Francesco, P. Faccioli, B. Galinhas, M. Gallinaro, J. Hollar, N. Leonardo, T. Niknejad, J. Seixas, K. Shchelina, G. Strong, O. Toldaiev, J. Varela

Joint Institute for Nuclear Research, Dubna, Russia
S. Afanasiev, P. Bunin, M. Gavrilenko, I. Golutvin, I. Gorbunov, A. Kamenev, V. Karjavine, A. Lanev, A. Malakhov, V. Matveev[37,38], P. Moisenz, V. Palichik, V. Perelygin, M. Savina, S. Shmatov, S. Shulha, N. Skatchkov, V. Smirnov, N. Voytishin, A. Zarubin

Petersburg Nuclear Physics Institute, Gatchina (St. Petersburg), Russia
L. Chtchipounov, V. Golovtcov, Y. Ivanov, V. Kim[39], E. Kuznetsova[40], P. Levchenko, V. Murzin, V. Oreshkin, I. Smirnov, D. Sosnov, V. Sulimov, L. Uvarov, A. Vorobyev

Institute for Nuclear Research, Moscow, Russia
Yu. Andreev, A. Dermenev, S. Gninenko, N. Golubev, A. Karneyeu, M. Kirsanov, N. Krasnikov, A. Pashenkov, D. Tlisov, A. Toropin

Institute for Theoretical and Experimental Physics named by A.I. Alikhanov of NRC 'Kurchatov Institute', Moscow, Russia
V. Epshteyn, V. Gavrilov, N. Lychkovskaya, A. Nikitenko[41], V. Popov, I. Pozdnyakov, G. Safronov, A. Spiridonov, A. Stepennov, M. Toms, E. Vlasov, A. Zhokin

Moscow Institute of Physics and Technology, Moscow, Russia
T. Aushev

National Research Nuclear University 'Moscow Engineering Physics Institute' (MEPhI), Moscow, Russia
P. Parygin, D. Philippov, E. Popova, V. Rusinov, E. Zhemchugov

P.N. Lebedev Physical Institute, Moscow, Russia
V. Andreev, M. Azarkin, I. Dremin, M. Kirakosyan, A. Terkulov

Skobeltsyn Institute of Nuclear Physics, Lomonosov Moscow State University, Moscow, Russia
A. Belyaev, E. Boos, M. Dubinin[42], L. Dudko, A. Ershov, A. Gribushin, V. Klyukhin, O. Kodolova, I. Lokhtin, S. Obraztsov, S. Petrushanko, V. Savrin, A. Snigirev

Novosibirsk State University (NSU), Novosibirsk, Russia
A. Barnyakov[43], V. Blinov[43], T. Dimova[43], L. Kardapoltsev[43], Y. Skovpen[43]

JHEP06(2020)018

Institute for High Energy Physics of National Research Centre 'Kurchatov Institute', Protvino, Russia

I. Azhgirey, I. Bayshev, S. Bitioukov, V. Kachanov, D. Konstantinov, P. Mandrik, V. Petrov, R. Ryutin, S. Slabospitskii, A. Sobol, S. Troshin, N. Tyurin, A. Uzunian, A. Volkov

National Research Tomsk Polytechnic University, Tomsk, Russia

A. Babaev, A. Iuzhakov, V. Okhotnikov

Tomsk State University, Tomsk, Russia

V. Borchsh, V. Ivanchenko, E. Tcherniaev

University of Belgrade: Faculty of Physics and VINCA Institute of Nuclear Sciences

P. Adzic[44], P. Cirkovic, M. Dordevic, P. Milenovic, J. Milosevic, M. Stojanovic

Centro de Investigaciones Energéticas Medioambientales y Tecnológicas (CIEMAT), Madrid, Spain

M. Aguilar-Benitez, J. Alcaraz Maestre, A. Álvarez Fernández, I. Bachiller, M. Barrio Luna, CristinaF. Bedoya, J.A. Brochero Cifuentes, C.A. Carrillo Montoya, M. Cepeda, M. Cerrada, N. Colino, B. De La Cruz, A. Delgado Peris, J.P. Fernández Ramos, J. Flix, M.C. Fouz, O. Gonzalez Lopez, S. Goy Lopez, J.M. Hernandez, M.I. Josa, D. Moran, Á. Navarro Tobar, A. Pérez-Calero Yzquierdo, J. Puerta Pelayo, I. Redondo, L. Romero, S. Sánchez Navas, M.S. Soares, A. Triossi, C. Willmott

Universidad Autónoma de Madrid, Madrid, Spain

C. Albajar, J.F. de Trocóniz, R. Reyes-Almanza

Universidad de Oviedo, Instituto Universitario de Ciencias y Tecnologías Espaciales de Asturias (ICTEA), Oviedo, Spain

B. Alvarez Gonzalez, J. Cuevas, C. Erice, J. Fernandez Menendez, S. Folgueras, I. Gonzalez Caballero, J.R. González Fernández, E. Palencia Cortezon, C. Ramón Álvarez, V. Rodríguez Bouza, S. Sanchez Cruz

Instituto de Física de Cantabria (IFCA), CSIC-Universidad de Cantabria, Santander, Spain

I.J. Cabrillo, A. Calderon, B. Chazin Quero, J. Duarte Campderros, M. Fernandez, P.J. Fernández Manteca, A. García Alonso, G. Gomez, C. Martinez Rivero, P. Martinez Ruiz del Arbol, F. Matorras, J. Piedra Gomez, C. Prieels, F. Ricci-Tam, T. Rodrigo, A. Ruiz-Jimeno, L. Russo[45], L. Scodellaro, I. Vila, J.M. Vizan Garcia

University of Colombo, Colombo, Sri Lanka

K. Malagalage

University of Ruhuna, Department of Physics, Matara, Sri Lanka

W.G.D. Dharmaratna, N. Wickramage

JHEP06(2020)018

CERN, European Organization for Nuclear Research, Geneva, Switzerland

D. Abbaneo, B. Akgun, E. Auffray, G. Auzinger, J. Baechler, P. Baillon, A.H. Ball, D. Barney, J. Bendavid, M. Bianco, A. Bocci, P. Bortignon, E. Bossini, E. Brondolin, T. Camporesi, A. Caratelli, G. Cerminara, E. Chapon, G. Cucciati, D. d'Enterria, A. Dabrowski, N. Daci, V. Daponte, A. David, O. Davignon, A. De Roeck, M. Deile, R. Di Maria, M. Dobson, M. Dünser, N. Dupont, A. Elliott-Peisert, N. Emriskova, F. Fallavollita[46], D. Fasanella, S. Fiorendi, G. Franzoni, J. Fulcher, W. Funk, S. Giani, D. Gigi, K. Gill, F. Glege, L. Gouskos, M. Gruchala, M. Guilbaud, D. Gulhan, J. Hegeman, C. Heidegger, Y. Iiyama, V. Innocente, T. James, P. Janot, O. Karacheban[19], J. Kaspar, J. Kieseler, M. Krammer[1], N. Kratochwil, C. Lange, P. Lecoq, C. Lourenço, L. Malgeri, M. Mannelli, A. Massironi, F. Meijers, S. Mersi, E. Meschi, F. Moortgat, M. Mulders, J. Ngadiuba, J. Niedziela, S. Nourbakhsh, S. Orfanelli, L. Orsini, F. Pantaleo[16], L. Pape, E. Perez, M. Peruzzi, A. Petrilli, G. Petrucciani, A. Pfeiffer, M. Pierini, F.M. Pitters, D. Rabady, A. Racz, M. Rieger, M. Rovere, H. Sakulin, J. Salfeld-Nebgen, S. Scarfi, C. Schäfer, C. Schwick, M. Selvaggi, A. Sharma, P. Silva, W. Snoeys, P. Sphicas[47], J. Steggemann, S. Summers, V.R. Tavolaro, D. Treille, A. Tsirou, G.P. Van Onsem, A. Vartak, M. Verzetti, W. Xiao, W.D. Zeuner

Paul Scherrer Institut, Villigen, Switzerland

L. Caminada[48], K. Deiters, W. Erdmann, R. Horisberger, Q. Ingram, H.C. Kaestli, D. Kotlinski, U. Langenegger, T. Rohe

ETH Zurich — Institute for Particle Physics and Astrophysics (IPA), Zurich, Switzerland

M. Backhaus, P. Berger, N. Chernyavskaya, G. Dissertori, M. Dittmar, M. Donegà, C. Dorfer, T.A. Gómez Espinosa, C. Grab, D. Hits, W. Lustermann, R.A. Manzoni, M.T. Meinhard, F. Micheli, P. Musella, F. Nessi-Tedaldi, F. Pauss, G. Perrin, L. Perrozzi, S. Pigazzini, M.G. Ratti, M. Reichmann, C. Reissel, T. Reitenspiess, B. Ristic, D. Ruini, D.A. Sanz Becerra, M. Schönenberger, L. Shchutska, M.L. Vesterbacka Olsson, R. Wallny, D.H. Zhu

Universität Zürich, Zurich, Switzerland

T.K. Aarrestad, C. Amsler[49], C. Botta, D. Brzhechko, M.F. Canelli, A. De Cosa, R. Del Burgo, B. Kilminster, S. Leontsinis, V.M. Mikuni, I. Neutelings, G. Rauco, P. Robmann, K. Schweiger, Y. Takahashi, S. Wertz

National Central University, Chung-Li, Taiwan

C.M. Kuo, W. Lin, A. Roy, S.S. Yu

National Taiwan University (NTU), Taipei, Taiwan

P. Chang, Y. Chao, K.F. Chen, P.H. Chen, W.-S. Hou, Y.y. Li, R.-S. Lu, E. Paganis, A. Psallidas, A. Steen

Chulalongkorn University, Faculty of Science, Department of Physics, Bangkok, Thailand

B. Asavapibhop, C. Asawatangtrakuldee, N. Srimanobhas, N. Suwonjandee

JHEP06(2020)018

Çukurova University, Physics Department, Science and Art Faculty, Adana, Turkey

A. Bat, F. Boran, A. Celik[50], S. Damarseckin[51], Z.S. Demiroglu, F. Dolek, C. Dozen[52], I. Dumanoglu, G. Gokbulut, EmineGurpinar Guler[53], Y. Guler, I. Hos[54], C. Isik, E.E. Kangal[55], O. Kara, A. Kayis Topaksu, U. Kiminsu, G. Onengut, K. Ozdemir[56], S. Ozturk[57], A.E. Simsek, U.G. Tok, S. Turkcapar, I.S. Zorbakir, C. Zorbilmez

Middle East Technical University, Physics Department, Ankara, Turkey

B. Isildak[58], G. Karapinar[59], M. Yalvac

Bogazici University, Istanbul, Turkey

I.O. Atakisi, E. Gülmez, M. Kaya[60], O. Kaya[61], Ö. Özçelik, S. Tekten, E.A. Yetkin[62]

Istanbul Technical University, Istanbul, Turkey

A. Cakir, K. Cankocak[63], Y. Komurcu, S. Sen[64]

Istanbul University, Istanbul, Turkey

S. Cerci[65], B. Kaynak, S. Ozkorucuklu, D. Sunar Cerci[65]

Institute for Scintillation Materials of National Academy of Science of Ukraine, Kharkov, Ukraine

B. Grynyov

National Scientific Center, Kharkov Institute of Physics and Technology, Kharkov, Ukraine

L. Levchuk

University of Bristol, Bristol, United Kingdom

E. Bhal, S. Bologna, J.J. Brooke, D. Burns[66], E. Clement, D. Cussans, H. Flacher, J. Goldstein, G.P. Heath, H.F. Heath, L. Kreczko, B. Krikler, S. Paramesvaran, T. Sakuma, S. Seif El Nasr-Storey, V.J. Smith, J. Taylor, A. Titterton

Rutherford Appleton Laboratory, Didcot, United Kingdom

K.W. Bell, A. Belyaev[67], C. Brew, R.M. Brown, D.J.A. Cockerill, J.A. Coughlan, K. Harder, S. Harper, J. Linacre, K. Manolopoulos, D.M. Newbold, E. Olaiya, D. Petyt, T. Reis, T. Schuh, C.H. Shepherd-Themistocleous, A. Thea, I.R. Tomalin, T. Williams

Imperial College, London, United Kingdom

R. Bainbridge, P. Bloch, S. Bonomally, J. Borg, S. Breeze, O. Buchmuller, A. Bundock, GurpreetSingh CHAHAL[68], D. Colling, P. Dauncey, G. Davies, M. Della Negra, P. Everaerts, G. Hall, G. Iles, M. Komm, L. Lyons, A.-M. Magnan, S. Malik, A. Martelli, V. Milosevic, A. Morton, J. Nash[69], V. Palladino, M. Pesaresi, D.M. Raymond, A. Richards, A. Rose, E. Scott, C. Seez, A. Shtipliyski, M. Stoye, T. Strebler, A. Tapper, K. Uchida, T. Virdee[16], N. Wardle, D. Winterbottom, A.G. Zecchinelli, S.C. Zenz

Brunel University, Uxbridge, United Kingdom

J.E. Cole, P.R. Hobson, A. Khan, P. Kyberd, C.K. Mackay, I.D. Reid, L. Teodorescu, S. Zahid

JHEP06(2020)018

Baylor University, Waco, U.S.A.

A. Brinkerhoff, K. Call, B. Caraway, J. Dittmann, K. Hatakeyama, C. Madrid, B. McMaster, N. Pastika, C. Smith

Catholic University of America, Washington, DC, U.S.A.

R. Bartek, A. Dominguez, R. Uniyal, A.M. Vargas Hernandez

The University of Alabama, Tuscaloosa, U.S.A.

A. Buccilli, S.I. Cooper, S.V. Gleyzer, C. Henderson, P. Rumerio, C. West

Boston University, Boston, U.S.A.

A. Albert, D. Arcaro, Z. Demiragli, D. Gastler, C. Richardson, J. Rohlf, D. Sperka, D. Spitzbart, I. Suarez, L. Sulak, D. Zou

Brown University, Providence, U.S.A.

G. Benelli, B. Burkle, X. Coubez[17], D. Cutts, Y.t. Duh, M. Hadley, U. Heintz, J.M. Hogan[70], K.H.M. Kwok, E. Laird, G. Landsberg, K.T. Lau, J. Lee, M. Narain, S. Sagir[71], R. Syarif, E. Usai, W.Y. Wong, D. Yu, W. Zhang

University of California, Davis, Davis, U.S.A.

R. Band, C. Brainerd, R. Breedon, M. Calderon De La Barca Sanchez, M. Chertok, J. Conway, R. Conway, P.T. Cox, R. Erbacher, C. Flores, G. Funk, F. Jensen, W. Ko[†], O. Kukral, R. Lander, M. Mulhearn, D. Pellett, J. Pilot, M. Shi, D. Taylor, K. Tos, M. Tripathi, Z. Wang, F. Zhang

University of California, Los Angeles, U.S.A.

M. Bachtis, C. Bravo, R. Cousins, A. Dasgupta, A. Florent, J. Hauser, M. Ignatenko, N. Mccoll, W.A. Nash, S. Regnard, D. Saltzberg, C. Schnaible, B. Stone, V. Valuev

University of California, Riverside, Riverside, U.S.A.

K. Burt, Y. Chen, R. Clare, J.W. Gary, S.M.A. Ghiasi Shirazi, G. Hanson, G. Karapostoli, O.R. Long, N. Manganelli, M. Olmedo Negrete, M.I. Paneva, W. Si, S. Wimpenny, B.R. Yates, Y. Zhang

University of California, San Diego, La Jolla, U.S.A.

J.G. Branson, P. Chang, S. Cittolin, S. Cooperstein, N. Deelen, M. Derdzinski, J. Duarte, R. Gerosa, D. Gilbert, B. Hashemi, D. Klein, V. Krutelyov, J. Letts, M. Masciovecchio, S. May, S. Padhi, M. Pieri, V. Sharma, M. Tadel, F. Würthwein, A. Yagil, G. Zevi Della Porta

University of California, Santa Barbara — Department of Physics, Santa Barbara, U.S.A.

N. Amin, R. Bhandari, C. Campagnari, M. Citron, V. Dutta, J. Incandela, B. Marsh, H. Mei, A. Ovcharova, H. Qu, J. Richman, U. Sarica, D. Stuart, S. Wang

California Institute of Technology, Pasadena, U.S.A.

D. Anderson, A. Bornheim, O. Cerri, I. Dutta, J.M. Lawhorn, N. Lu, J. Mao, H.B. Newman, T.Q. Nguyen, J. Pata, M. Spiropulu, J.R. Vlimant, S. Xie, Z. Zhang, R.Y. Zhu

JHEP06(2020)018

Carnegie Mellon University, Pittsburgh, U.S.A.

M.B. Andrews, T. Ferguson, T. Mudholkar, M. Paulini, M. Sun, I. Vorobiev, M. Weinberg

University of Colorado Boulder, Boulder, U.S.A.

J.P. Cumalat, W.T. Ford, E. MacDonald, T. Mulholland, R. Patel, A. Perloff, K. Stenson, K.A. Ulmer, S.R. Wagner

Cornell University, Ithaca, U.S.A.

J. Alexander, Y. Cheng, J. Chu, A. Datta, A. Frankenthal, K. Mcdermott, J.R. Patterson, D. Quach, A. Ryd, S.M. Tan, Z. Tao, J. Thom, P. Wittich, M. Zientek

Fermi National Accelerator Laboratory, Batavia, U.S.A.

S. Abdullin, M. Albrow, M. Alyari, G. Apollinari, A. Apresyan, A. Apyan, S. Banerjee, L.A.T. Bauerdick, A. Beretvas, D. Berry, J. Berryhill, P.C. Bhat, K. Burkett, J.N. Butler, A. Canepa, G.B. Cerati, H.W.K. Cheung, F. Chlebana, M. Cremonesi, V.D. Elvira, J. Freeman, Z. Gecse, E. Gottschalk, L. Gray, D. Green, S. Grünendahl, O. Gutsche, J. Hanlon, R.M. Harris, S. Hasegawa, R. Heller, J. Hirschauer, B. Jayatilaka, S. Jindariani, M. Johnson, U. Joshi, T. Klijnsma, B. Klima, M.J. Kortelainen, B. Kreis, S. Lammel, J. Lewis, D. Lincoln, R. Lipton, M. Liu, T. Liu, J. Lykken, K. Maeshima, J.M. Marraffino, D. Mason, P. McBride, P. Merkel, S. Mrenna, S. Nahn, V. O'Dell, V. Papadimitriou, K. Pedro, C. Pena[42], F. Ravera, A. Reinsvold Hall, L. Ristori, B. Schneider, E. Sexton-Kennedy, N. Smith, A. Soha, W.J. Spalding, L. Spiegel, S. Stoynev, J. Strait, L. Taylor, S. Tkaczyk, N.V. Tran, L. Uplegger, E.W. Vaandering, C. Vernieri, R. Vidal, M. Wang, H.A. Weber, A. Woodard

University of Florida, Gainesville, U.S.A.

D. Acosta, P. Avery, D. Bourilkov, L. Cadamuro, V. Cherepanov, F. Errico, R.D. Field, D. Guerrero, B.M. Joshi, M. Kim, J. Konigsberg, A. Korytov, K.H. Lo, K. Matchev, N. Menendez, G. Mitselmakher, D. Rosenzweig, K. Shi, J. Wang, S. Wang, X. Zuo

Florida International University, Miami, U.S.A.

Y.R. Joshi

Florida State University, Tallahassee, U.S.A.

T. Adams, A. Askew, S. Hagopian, V. Hagopian, K.F. Johnson, R. Khurana, T. Kolberg, G. Martinez, T. Perry, H. Prosper, C. Schiber, R. Yohay, J. Zhang

Florida Institute of Technology, Melbourne, U.S.A.

M.M. Baarmand, M. Hohlmann, D. Noonan, M. Rahmani, M. Saunders, F. Yumiceva

University of Illinois at Chicago (UIC), Chicago, U.S.A.

M.R. Adams, L. Apanasevich, R.R. Betts, R. Cavanaugh, X. Chen, S. Dittmer, O. Evdokimov, C.E. Gerber, D.A. Hangal, D.J. Hofman, V. Kumar, C. Mills, T. Roy, M.B. Tonjes, N. Varelas, J. Viinikainen, H. Wang, X. Wang, Z. Wu

The University of Iowa, Iowa City, U.S.A.

M. Alhusseini, B. Bilki[53], K. Dilsiz[72], S. Durgut, R.P. Gandrajula, M. Haytmyradov, V. Khristenko, O.K. Köseyan, J.-P. Merlo, A. Mestvirishvili[73], A. Moeller, J. Nachtman, H. Ogul[74], Y. Onel, F. Ozok[75], A. Penzo, C. Snyder, E. Tiras, J. Wetzel, K. Yi[76]

JHEP06(2020)018

Johns Hopkins University, Baltimore, U.S.A.

B. Blumenfeld, A. Cocoros, N. Eminizer, A.V. Gritsan, W.T. Hung, S. Kyriacou, P. Maksimovic, J. Roskes, M. Swartz, T.Á. Vámi

The University of Kansas, Lawrence, U.S.A.

C. Baldenegro Barrera, P. Baringer, A. Bean, S. Boren, A. Bylinkin, T. Isidori, S. Khalil, J. King, G. Krintiras, A. Kropivnitskaya, C. Lindsey, D. Majumder, W. Mcbrayer, N. Minafra, M. Murray, C. Rogan, C. Royon, S. Sanders, E. Schmitz, J.D. Tapia Takaki, Q. Wang, J. Williams, G. Wilson

Kansas State University, Manhattan, U.S.A.

S. Duric, A. Ivanov, K. Kaadze, D. Kim, Y. Maravin, D.R. Mendis, T. Mitchell, A. Modak, A. Mohammadi

Lawrence Livermore National Laboratory, Livermore, U.S.A.

F. Rebassoo, D. Wright

University of Maryland, College Park, U.S.A.

A. Baden, O. Baron, A. Belloni, S.C. Eno, Y. Feng, N.J. Hadley, S. Jabeen, G.Y. Jeng, R.G. Kellogg, A.C. Mignerey, S. Nabili, M. Seidel, Y.H. Shin, A. Skuja, S.C. Tonwar, L. Wang, K. Wong

Massachusetts Institute of Technology, Cambridge, U.S.A.

D. Abercrombie, B. Allen, R. Bi, S. Brandt, W. Busza, I.A. Cali, M. D'Alfonso, G. Gomez Ceballos, M. Goncharov, P. Harris, D. Hsu, M. Hu, M. Klute, D. Kovalskyi, Y.-J. Lee, P.D. Luckey, B. Maier, A.C. Marini, C. Mcginn, C. Mironov, S. Narayanan, X. Niu, C. Paus, D. Rankin, C. Roland, G. Roland, Z. Shi, G.S.F. Stephans, K. Sumorok, K. Tatar, D. Velicanu, J. Wang, T.W. Wang, B. Wyslouch

University of Minnesota, Minneapolis, U.S.A.

R.M. Chatterjee, A. Evans, S. Guts†, P. Hansen, J. Hiltbrand, Sh. Jain, Y. Kubota, Z. Lesko, J. Mans, M. Revering, R. Rusack, R. Saradhy, N. Schroeder, N. Strobbe, M.A. Wadud

University of Mississippi, Oxford, U.S.A.

J.G. Acosta, S. Oliveros

University of Nebraska-Lincoln, Lincoln, U.S.A.

K. Bloom, S. Chauhan, D.R. Claes, C. Fangmeier, L. Finco, F. Golf, R. Kamalieddin, I. Kravchenko, J.E. Siado, G.R. Snow†, B. Stieger, W. Tabb

State University of New York at Buffalo, Buffalo, U.S.A.

G. Agarwal, C. Harrington, I. Iashvili, A. Kharchilava, C. McLean, D. Nguyen, A. Parker, J. Pekkanen, S. Rappoccio, B. Roozbahani

Northeastern University, Boston, U.S.A.

G. Alverson, E. Barberis, C. Freer, Y. Haddad, A. Hortiangtham, G. Madigan, B. Marzocchi, D.M. Morse, T. Orimoto, L. Skinnari, A. Tishelman-Charny, T. Wamorkar, B. Wang, A. Wisecarver, D. Wood

JHEP06(2020)018

Northwestern University, Evanston, U.S.A.

S. Bhattacharya, J. Bueghly, G. Fedi, A. Gilbert, T. Gunter, K.A. Hahn, N. Odell, M.H. Schmitt, K. Sung, M. Velasco

University of Notre Dame, Notre Dame, U.S.A.

R. Bucci, N. Dev, R. Goldouzian, M. Hildreth, K. Hurtado Anampa, C. Jessop, D.J. Karmgard, K. Lannon, W. Li, N. Loukas, N. Marinelli, I. Mcalister, F. Meng, Y. Musienko[37], R. Ruchti, P. Siddireddy, G. Smith, S. Taroni, M. Wayne, A. Wightman, M. Wolf

The Ohio State University, Columbus, U.S.A.

J. Alimena, B. Bylsma, L.S. Durkin, B. Francis, C. Hill, W. Ji, A. Lefeld, T.Y. Ling, B.L. Winer

Princeton University, Princeton, U.S.A.

G. Dezoort, P. Elmer, J. Hardenbrook, N. Haubrich, S. Higginbotham, A. Kalogeropoulos, S. Kwan, D. Lange, M.T. Lucchini, J. Luo, D. Marlow, K. Mei, I. Ojalvo, J. Olsen, C. Palmer, P. Piroué, D. Stickland, C. Tully

University of Puerto Rico, Mayaguez, U.S.A.

S. Malik, S. Norberg

Purdue University, West Lafayette, U.S.A.

A. Barker, V.E. Barnes, R. Chawla, S. Das, L. Gutay, M. Jones, A.W. Jung, B. Mahakud, D.H. Miller, G. Negro, N. Neumeister, C.C. Peng, S. Piperov, H. Qiu, J.F. Schulte, N. Trevisani, F. Wang, R. Xiao, W. Xie

Purdue University Northwest, Hammond, U.S.A.

T. Cheng, J. Dolen, N. Parashar

Rice University, Houston, U.S.A.

A. Baty, U. Behrens, S. Dildick, K.M. Ecklund, S. Freed, F.J.M. Geurts, M. Kilpatrick, Arun Kumar, W. Li, B.P. Padley, R. Redjimi, J. Roberts, J. Rorie, W. Shi, A.G. Stahl Leiton, Z. Tu, A. Zhang

University of Rochester, Rochester, U.S.A.

A. Bodek, P. de Barbaro, R. Demina, J.L. Dulemba, C. Fallon, T. Ferbel, M. Galanti, A. Garcia-Bellido, O. Hindrichs, A. Khukhunaishvili, E. Ranken, R. Taus

Rutgers, The State University of New Jersey, Piscataway, U.S.A.

B. Chiarito, J.P. Chou, A. Gandrakota, Y. Gershtein, E. Halkiadakis, A. Hart, M. Heindl, E. Hughes, S. Kaplan, I. Laflotte, A. Lath, R. Montalvo, K. Nash, M. Osherson, S. Salur, S. Schnetzer, S. Somalwar, R. Stone, S. Thomas

University of Tennessee, Knoxville, U.S.A.

H. Acharya, A.G. Delannoy, S. Spanier

JHEP06(2020)018

Texas A&M University, College Station, U.S.A.

O. Bouhali[77], M. Dalchenko, M. De Mattia, A. Delgado, R. Eusebi, J. Gilmore, T. Huang, T. Kamon[78], H. Kim, S. Luo, S. Malhotra, D. Marley, R. Mueller, D. Overton, L. Perniè, D. Rathjens, A. Safonov

Texas Tech University, Lubbock, U.S.A.

N. Akchurin, J. Damgov, F. De Guio, V. Hegde, S. Kunori, K. Lamichhane, S.W. Lee, T. Mengke, S. Muthumuni, T. Peltola, S. Undleeb, I. Volobouev, Z. Wang, A. Whitbeck

Vanderbilt University, Nashville, U.S.A.

S. Greene, A. Gurrola, R. Janjam, W. Johns, C. Maguire, A. Melo, H. Ni, K. Padeken, F. Romeo, P. Sheldon, S. Tuo, J. Velkovska, M. Verweij

University of Virginia, Charlottesville, U.S.A.

M.W. Arenton, P. Barria, B. Cox, G. Cummings, J. Hakala, R. Hirosky, M. Joyce, A. Ledovskoy, C. Neu, B. Tannenwald, Y. Wang, E. Wolfe, F. Xia

Wayne State University, Detroit, U.S.A.

R. Harr, P.E. Karchin, N. Poudyal, J. Sturdy, P. Thapa

University of Wisconsin — Madison, Madison, WI, U.S.A.

K. Black, T. Bose, J. Buchanan, C. Caillol, D. Carlsmith, S. Dasu, I. De Bruyn, L. Dodd, C. Galloni, H. He, M. Herndon, A. Hervé, U. Hussain, A. Lanaro, A. Loeliger, K. Long, R. Loveless, J. Madhusudanan Sreekala, A. Mallampalli, D. Pinna, T. Ruggles, A. Savin, V. Sharma, W.H. Smith, D. Teague, S. Trembath-reichert

†: Deceased
1: Also at Vienna University of Technology, Vienna, Austria
2: Also at IRFU, CEA, Université Paris-Saclay, Gif-sur-Yvette, France
3: Also at Universidade Estadual de Campinas, Campinas, Brazil
4: Also at Federal University of Rio Grande do Sul, Porto Alegre, Brazil
5: Also at UFMS, Nova Andradina, Brazil
6: Also at Universidade Federal de Pelotas, Pelotas, Brazil
7: Also at Université Libre de Bruxelles, Bruxelles, Belgium
8: Also at University of Chinese Academy of Sciences, Beijing, China
9: Also at Institute for Theoretical and Experimental Physics named by A.I. Alikhanov of NRC 'Kurchatov Institute', Moscow, Russia
10: Also at Joint Institute for Nuclear Research, Dubna, Russia
11: Also at Suez University, Suez, Egypt
12: Now at British University in Egypt, Cairo, Egypt
13: Also at Purdue University, West Lafayette, U.S.A.
14: Also at Université de Haute Alsace, Mulhouse, France
15: Also at Erzincan Binali Yildirim University, Erzincan, Turkey
16: Also at CERN, European Organization for Nuclear Research, Geneva, Switzerland
17: Also at RWTH Aachen University, III. Physikalisches Institut A, Aachen, Germany
18: Also at University of Hamburg, Hamburg, Germany
19: Also at Brandenburg University of Technology, Cottbus, Germany
20: Also at Institute of Physics, University of Debrecen, Debrecen, Hungary, Debrecen, Hungary

JHEP06(2020)018

21: Also at Institute of Nuclear Research ATOMKI, Debrecen, Hungary
22: Also at MTA-ELTE Lendület CMS Particle and Nuclear Physics Group, Eötvös Loránd University, Budapest, Hungary, Budapest, Hungary
23: Also at IIT Bhubaneswar, Bhubaneswar, India, Bhubaneswar, India
24: Also at Institute of Physics, Bhubaneswar, India
25: Also at G.H.G. Khalsa College, Punjab, India
26: Also at Shoolini University, Solan, India
27: Also at University of Hyderabad, Hyderabad, India
28: Also at University of Visva-Bharati, Santiniketan, India
29: Now at INFN Sezione di Bari[a], Università di Bari[b], Politecnico di Bari[c], Bari, Italy
30: Also at Italian National Agency for New Technologies, Energy and Sustainable Economic Development, Bologna, Italy
31: Also at Centro Siciliano di Fisica Nucleare e di Struttura Della Materia, Catania, Italy
32: Also at Scuola Normale e Sezione dell'INFN, Pisa, Italy
33: Also at Riga Technical University, Riga, Latvia, Riga, Latvia
34: Also at Malaysian Nuclear Agency, MOSTI, Kajang, Malaysia
35: Also at Consejo Nacional de Ciencia y Tecnología, Mexico City, Mexico
36: Also at Warsaw University of Technology, Institute of Electronic Systems, Warsaw, Poland
37: Also at Institute for Nuclear Research, Moscow, Russia
38: Now at National Research Nuclear University 'Moscow Engineering Physics Institute' (MEPhI), Moscow, Russia
39: Also at St. Petersburg State Polytechnical University, St. Petersburg, Russia
40: Also at University of Florida, Gainesville, U.S.A.
41: Also at Imperial College, London, United Kingdom
42: Also at California Institute of Technology, Pasadena, U.S.A.
43: Also at Budker Institute of Nuclear Physics, Novosibirsk, Russia
44: Also at Faculty of Physics, University of Belgrade, Belgrade, Serbia
45: Also at Università degli Studi di Siena, Siena, Italy
46: Also at INFN Sezione di Pavia[a], Università di Pavia[b], Pavia, Italy, Pavia, Italy
47: Also at National and Kapodistrian University of Athens, Athens, Greece
48: Also at Universität Zürich, Zurich, Switzerland
49: Also at Stefan Meyer Institute for Subatomic Physics, Vienna, Austria, Vienna, Austria
50: Also at Burdur Mehmet Akif Ersoy University, BURDUR, Turkey
51: Also at Şırnak University, Sirnak, Turkey
52: Also at Department of Physics, Tsinghua University, Beijing, China, Beijing, China
53: Also at Beykent University, Istanbul, Turkey, Istanbul, Turkey
54: Also at Istanbul Aydin University, Application and Research Center for Advanced Studies (App. & Res. Cent. for Advanced Studies), Istanbul, Turkey
55: Also at Mersin University, Mersin, Turkey
56: Also at Piri Reis University, Istanbul, Turkey
57: Also at Gaziosmanpasa University, Tokat, Turkey
58: Also at Ozyegin University, Istanbul, Turkey
59: Also at Izmir Institute of Technology, Izmir, Turkey
60: Also at Marmara University, Istanbul, Turkey
61: Also at Kafkas University, Kars, Turkey
62: Also at Istanbul Bilgi University, Istanbul, Turkey
63: Also at Near East University, Research Center of Experimental Health Science, Nicosia, Turkey

JHEP06(2020)018

64: Also at Hacettepe University, Ankara, Turkey
65: Also at Adiyaman University, Adiyaman, Turkey
66: Also at Vrije Universiteit Brussel, Brussel, Belgium
67: Also at School of Physics and Astronomy, University of Southampton, Southampton, United Kingdom
68: Also at IPPP Durham University, Durham, United Kingdom
69: Also at Monash University, Faculty of Science, Clayton, Australia
70: Also at Bethel University, St. Paul, Minneapolis, U.S.A., St. Paul, U.S.A.
71: Also at Karamanoğlu Mehmetbey University, Karaman, Turkey
72: Also at Bingol University, Bingol, Turkey
73: Also at Georgian Technical University, Tbilisi, Georgia
74: Also at Sinop University, Sinop, Turkey
75: Also at Mimar Sinan University, Istanbul, Istanbul, Turkey
76: Also at Nanjing Normal University Department of Physics, Nanjing, China
77: Also at Texas A&M University at Qatar, Doha, Qatar
78: Also at Kyungpook National University, Daegu, Korea, Daegu, Korea

JHEP06(2020)018